3-8-2004

Flow Around an Object Projected from a Cavity into a Supersonic Freestream

Scott T. Bjorge

Follow this and additional works at: https://scholar.afit.edu/etd

Part of the Aerodynamics and Fluid Mechanics Commons

FLOW AROUND AN OBJECT PROJECTED FROM A CAVITY
INTO A SUPERSONIC FREESTREAM

THESIS

Scott T. Bjorge, Captain, USAF

AFIT/GAE/ENY/04-M02

DEPARTMENT OF THE AIR FORCE
AIR UNIVERSITY

AIR FORCE INSTITUTE OF TECHNOLOGY

Wright-Patterson Air Force Base, Ohio

APPROVED FOR PUBLIC RELEASE; DISTRIBUTION UNLIMITED

AFIT/GAE/ENY/04-M02

FLOW AROUND AN OBJECT PROJECTED FROM A CAVITY
INTO A SUPERSONIC FREESTREAM

THESIS

Presented to the Faculty

Department of Aeronautics and Astronautics

Graduate School of Engineering and Management

Air Force Institute of Technology

Air University

Air Education and Training Command

In Partial Fulfillment of the Requirements for the

Degree of Master of Science in Aeronautical Engineering

Scott T. Bjorge, BS

Captain, USAF

March 2004

APPROVED FOR PUBLIC RELEASE; DISTRIBUTION UNLIMITED

AFIT/GAE/ENY/04-M02

FLOW AROUND AN OBJECT PROJECTED FROM A CAVITY
INTO A SUPERSONIC FREESTREAM

Scott T. Bjorge, BS
Captain, USAF

Approved:

_____//signed//_____   _8 Mar 04
Dr. Mark F. Reeder (Chairman)   Date

_____//signed//_____   _8 Mar 04
Raymond C. Maple, Lt Col, USAF (Member)   Date

_____//signed//_____   __9 Mar 04
Eric J. Stephen, Lt Col, USAF (Member)   Date

AFIT/GAE/ENY/04-M02

Abstract

       The pressure and flow field of a supersonic flow over a cavity, with and without a store, was the focus of this experimental investigation. A single cavity geometry, with a length to depth ratio of 3.6 was studied while the freestream Mach number and the placement of the store relative to the cavity floor were varied.

       The traits of the pressure spectra on the cavity floor were markedly different between freestream Mach numbers of 1.8 and 2.9. While the Mach 1.8 case exhibited clear spectral peaks consistent with predictions by Rossiter, the Mach 2.9 flow field did not. With the store placed within the free shear layer, the level of pressure fluctuations measured on the cavity floor decreased for the Mach 1.8 case and increased for the Mach 2.9 case.

       High-speed Schlieren photography was used to visualize the interaction of the free shear layer and the modeled store. Images revealed that flow structures in the free shear layer of the Mach 2.9 flow exhibited less spanwise coherence than their Mach 1.8 flow counterparts. Images also revealed vertical displacement of the free shear layer as the store traversed through it.

       Pressure-sensitive paint (PSP) was utilized to quantify the full-field mean pressure on the cavity floor and store. A pressure rise near the trailing edge was noted for both freestream Mach numbers. The mean pressure contour of the floor for the Mach 1.8 case exhibited considerable three-dimensionality, despite the generally spanwise coherent structures in the free shear layer. The store exhibited asymmetry in the pressure field and

a strong dependence on its vertical position. The pressure fields were then integrated over

the area of the store, resulting in the calculation of the aerodynamic coefficients.

To my parents for their strength and guidance over the years

Acknowledgments

I would like to express my deep gratitude to my faculty advisor, Dr. Mark Reeder, for his guidance and support throughout the course of this thesis effort. The knowledge he shared with me was instrumental to the success of this project. His ability to keep me headed in right direction and his tales of the second best football team in the land will not be forgotten. To Mr. Jan LeValley of the AFIT Model Shop, who expertly crafted much of the experimental set-up and took on the daunting task of pressure sensitive paint with me. To Dr. Sergey Fonov, who patiently guided me through software tutorials and facilitated the PSP image processing. Last, I would like to thank Mr. Andrew Pitts for without his expertise this project would not have been possible. He was always there to lend a hand, smile, and offer a lesson on life.

<div align="center">Scott T. Bjorge</div>

Table of Contents

List of Figures

List of Tables

FLOW AROUND AN OBJECT PROJECTED FROM A CAVITY

INTO A SUPERSONIC FREESTREAM

I. Introduction

Section 1 - Motivation

Internal weapons bays on military aircraft have a number of design advantages in comparison to external stores. A short list of these advantages include: elimination of aerodynamic heating of the store, lower radar cross-section and reduced aerodynamic drag, which directly leads to increased maneuverability and range (5:1).

However, internal weapons bays are not without negatives, which can be magnified when supersonic store release speeds are desired. These side-effects present themselves at the beginning of the store release cycle. Once the weapon bay doors are opened, the geometry of the cavity and the freestream flow conditions dictate the resultant flow dynamics over the cavity. One of the most common phenomena is the formation of self-sustaining pressure oscillations, creating cavity resonance, which can lead to structural fatigue of the aircraft and the store and extensive damage to sensitive store electronics. The second major concern occurs when the store is released and interacts with the unsteady airflow present in the dynamic shear layer formed over the cavity. Unpredictable motion of the released store can be directly attributed to this shear layer interaction, which could lead to the store missing its intended target or even aircraft damage. Another concern is the traversing of the store through the shock that is formed at the leading edge of the cavity, which can also lead to unpredictable store motion. For

1

these reasons, modern aircraft with internal weapons bays typically decelerate to subsonic speeds prior to store release, greatly increasing the vulnerability of the aircraft.

Engineers have successfully integrated aircraft and stores for subsonic store release, since they have been in use for decades, and there hasn't been an overwhelming need for supersonic stores release. However, as the targeting capabilities of hostile parties increase over time, the requirement that an aircraft slow down prior to store release could have serious consequences. For this reason support is growing for a supersonic strike aircraft.

To achieve a successful munitions release all components essential to the separation process must be integrated correctly. The three main components are the aircraft (and the subsequent design of the weapons bay or cavity), the store ejector system and the store itself. The design of a new aircraft incorporates the ability to utilize stores currently in use or under production, but over the life of the aircraft munitions evolve and new munitions become available. On the other hand, munitions designers are concentrating on making the best, most reliable munition available. Over the life span of the aircraft and the munition, it is quite possible combat stores configurations could evolve into a combination not envisioned by the designers of either component. The design of the ejector system used to push the stores from the weapons bay and safely away from the aircraft is also integral to release.

There have been a number of published studies of the aerodynamics of stores in a supersonic flow (9; 26), and there have been numerous studies on the effects of supersonic flow over a cavity and the attempt to control it (5; 24; 25), but there have been

few studies of the integration of the store and the cavity (2). Since the ultimate goal is to provide advanced stores, released from advanced aircraft in an accurate and predictable manner, the intent of this experiment is to improve the understanding of the interaction of the store and cavity exposed to a supersonic freestream as a system.

Section 2 - Research Focus and Goals

As stated earlier, there have been very few studies that have examined the interaction of the cavity and the store as a system. This raises many questions about the effect the store has on the flow characteristics of a cavity, particularly in supersonic flow. The following paragraphs will lay the foundation for the reasoning behind the experimental set-up and data acquisition methods and techniques. They will also provide a path leading to the overall goals of the experiment.

The focus of this experimental procedure was to characterize aspects of supersonic flow over a cavity and to study the interaction of a simulated store exiting the cavity and its effect on the flow around the cavity. A single cavity with a length to depth ratio of 3.6 (L/D=3.6) and a single store geometry were tested in AFIT's supersonic blowdown wind tunnel facility. Freestream conditions of Mach 1.8 and Mach 2.9 were explored. Data was obtained with an array of high-speed pressure transducers, pressure sensitive paint (PSP), and Schlieren photography.

The array of five high-speed pressure transducers served two important functions. First, they were used to obtain the fluctuating pressures present on the cavity floor during testing. Given the cavity geometry and from existing literature, it was expected the high-speed pressure transducers would capture the self sustaining frequency oscillations

3

produced by the high-speed flow over the cavity. Once the baseline oscillations were known, the next step was to determine if the presence of the store had any effect on the oscillations. The effect of a change in freestream Mach number was also explored. Second, the transducers were used extensively in conjunction with the PSP for calibration of the PSP and data verification.

The placement of the transducers on the floor of the cavity served several purposes. First, mounting on the cavity floor locates the transducers in proximity to the PSP painted surface, making it an ideal setting for the in-situ calibration that will be explained in detail in Chapter III. Second, the placement of the transducers could be similar to the placement one might expect in a flow control feedback system, where pressure data provides the basis for the oscillation of the active flow control device. Another important reason is the availability of other published cavity flow data that also used pressure transducers located on the cavity floor, allowing for comparison.

The key advantage of a pressure sensitive paint system is its ability to provide a global mapping of the pressure levels over an entire surface non-intrusively. The only change to the geometry of the test surface is a thin layer (10-15 µm) of paint (19). Developed in the 1980's in the former Soviet Union, PSP has continued to evolve. Early PSP coatings were not very sensitive and were highly temperature dependent (3:158). But newer paints have been developed that exhibit negligible temperature sensitivity over a large range of temperature operation conditions. Figure 1 shows a sample painted with PSP and a visualization of the resulting pressure distribution that results after image

processing. The technology behind PSP as well as the specific paint used in this experiment will be discussed in Chapter II and Chapter III, respectively.
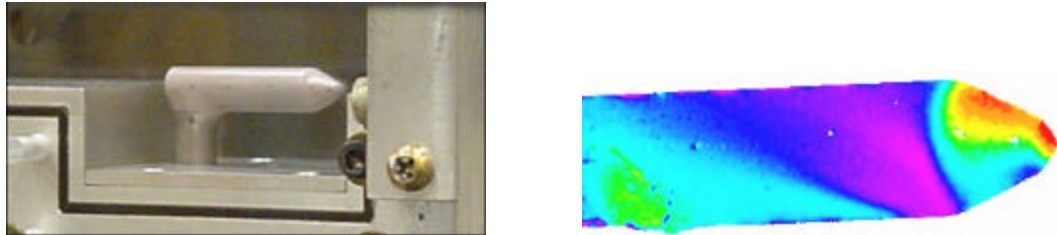
Figure 1. (a) Sample painted with PSP and (b) Resulting pressure output

The PSP was applied to the cavity floor and to the simulated store. The floor was painted for two reasons. First, it allowed the pressure measurement of the entire cavity floor, since the pressure transducers only measured specific locations. Second, as mentioned before, the combination of the PSP and the pressure transducers at the same location allowed direct calibration of the PSP. The simple geometry of the cavity floor provided the additional benefit of facilitating the PSP data processing since these are initial tests with this system. In the future, as PSP and camera technology continue to improve, the mean pressures determined here will also provide a baseline to compare fluctuating pressures measured using time-accurate PSP.

The store was painted primarily due to the difficulty of installing multiple pressure transducers on the store. Pressure data on the store was desired to provide baseline data to be used to accurately characterize the pressure field encountered by the store. The results here lend considerable insight into the pressures acting on the store at

various vertical locations. In turn, this pressure field can be used to calculate the aerodynamic coefficients to predict store trajectory. Again, this information is not readily available in existing literature. In addition, the pressure field could be used as a basis for comparison to computational fluid dynamics results. There is great future potential for improved forms of PSP to measure fluctuating pressures, which would allow actual release of a simulated store in a wind tunnel, which is nearly impossible with the use of pressure transducers and their associated wiring.

The use of pressure transducers and PSP reveals much about the interaction of the cavity and the store, but not the entire picture. The use of Schlieren photography provides a real-time visualization of the shear layer dynamics as well as the interaction of the simulated store and shear layer to help complete the picture. It is common in both literature and in practice to assume a pseudo steady shear layer for external store separation (15:938; 29:518), but serious questions arise as to whether this assumption is valid for internal store separation. The effect of compressibility on the shear layer, not to mention the store cavity system is also an open question. Likewise, as the store is introduced into the system, it may influence the shear layer. Schlieren photography is able to provide considerable insight into these issues.

Stated concisely, the overall goal of this experiment is to accurately characterize aspects of the interaction of a cavity and simulated store in a supersonic freestream flow. The experimental results gained from this experiment successfully led to increase understanding of the complex store-cavity interaction that occurs at supersonic speeds. Furthermore, this research provides benchmark global mean pressure data that could later

6

be compared to time-accurate PSP measurements or to cases where flow control devices are implemented to alleviate the undesirable characteristics of supersonic store release from a cavity.

Section 3 - Outline

This section provides an overview of the chapters to follow. Chapter II provides an overview of the aerodynamics associated with cavity flows and some previous results. It also presents the theoretical details of PSP. Chapter III details the experimental set-up used to conduct this study. In Chapter IV the results of the experiment are presented and analyzed. Finally, Chapter V includes conclusions and discusses possible future work.

II. Theoretical and Experimental Background

Section 1 - Flow Characteristics

Despite its geometric simplicity, flow over a cavity leads to a complex flow problem. The dynamics of the cavity flow problem are a function of the freestream flow conditions and the cavity geometry. The main areas of interest concerning cavity flow are the freestream flow, incoming boundary layer, shear layer, and the flow inside the cavity, all displayed in Figure 2 (16:847).
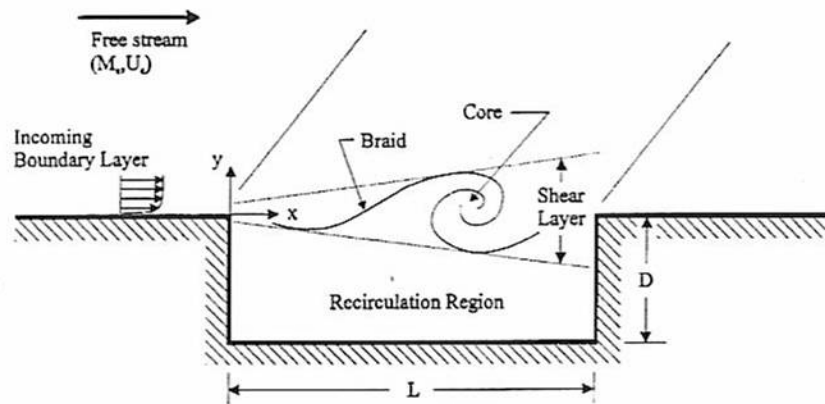
Figure 2. Compressible two-dimensional cavity flowfield. (16:847)

There are two main classifications for characterizing cavity flows: open and closed flow. As shown in Figure 3, the type of flow produced is a function of geometry. Closed flows are formed when the length to depth ratio is greater than 13, and open flows are for an L/D less than 10, with a transitional area between. For closed flows, the shear layer expands at the leading edge of the cavity and impinges on the floor of the cavity. Expansion waves are generated when supersonic flow is turned away from itself around a convex corner (1:130). Since the Mach number increases in an expansion wave, the

8

pressure decreases, resulting in initial pressure coefficient (C_p) at the upstream edge of the cavity shown in Figure 3. The entire trend of C_p for a closed flow is also shown in Figure 3.

For an open flow, an oblique shock, rather than an expansion, forms at the cavity's leading edge. The shear layer does not impinge on the cavity floor and exhibits a fairly constant C_p except near the trailing edge of the cavity. Of the two types of flows, an open flow situation exhibits more favorable store separation conditions (35:684). At an L/D of 3.6, the cavity in this experiment is expected to have open flow characteristics, which the collected data supports.

Closed cavity flow (L/D > 13)   Open Cavity Flow (L/D < 10)
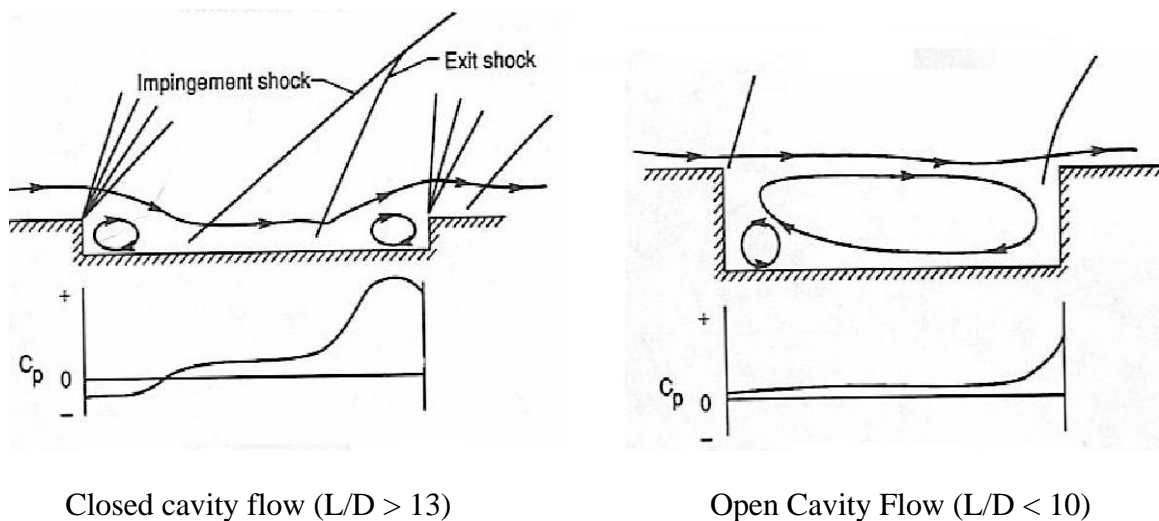
Figure 3. Classifications of cavity flows. (35:683)

The resultant characteristics of the flow internal to the cavity are dependent upon the freestream conditions, the incoming boundary layer, and the shear layer over the cavity. Open cavity flow is usually associated with high dynamic pressure loads on the

floor of the cavity (33:1). These dynamic pressure loads are the result vortex shedding, which is caused by unsteady flow in the shear layer (36:2). A simple description of the generation of a strong single-frequency tone in the cavity should be discussed. A Kelvin-Helmholtz (K-H) instability is formed at the point of interaction of flows of different velocities, in this case, the supersonic freestream and the subsonic flow inside the cavity. This K-H instability initiates a discrete spanwise vortex sheet at the leading edge of the cavity. As the vortex convects downstream, it grows and evolves until it reaches the trailing edge of the cavity whereupon it interacts with the downstream wall of the cavity and a pressure wave convects upstream through the subsonic flow within the cavity. This pressure wave stimulates the formation of another K-H vortex and the self-sustaining cycle, termed cavity resonance, is repeated. The resonant cavity falls in the same category of other fluid-resonant phenomena, such as the screech tone generated by an under expanded supersonic jet (21:1). The frequency of the cavity resonance is dominated by the cavity geometry and freestream velocity. A non-dimensional measurement of the frequency of the oscillations is the Strouhal number, defined as (22:157):

$$S_n = \frac{f_n L}{U}$$

Where S_n is the Strouhal number, f_n is the frequency, L is the length of the cavity, and U is the freestream velocity. To determine the Strouhal number, and subsequently the oscillation frequency (using known geometry and velocity), the Rossiter formula is used. Originally the Rossiter formula was defined as (12:548):

$$S_n = \frac{n - C_1}{M + \dfrac{1}{C_2}}$$

where, n is the mode of the frequency present ($n = 1, 2, 3\ldots$), and C_1 and C_2 are constants which have been experimentally determined to be 0.25 and 0.57 respectively (16:1). The values for n are often referred to as Rossiter modes.

The Rossiter formula was subsequently modified by Heller et. al. to improve accuracy at higher levels of compressibility by assuming the cavity speed of sound is equal to the freestream speed of sound (12:550). The preferred form of the Rossiter formula applied to compressible flow is the modified version defined as (22:157):

$$S_n = \frac{f_n L}{U} = \frac{n - C_1}{x + \dfrac{1}{C_2}}$$

where C_1, C_2 and n are as defined previously and ? is a function of Mach number defined as:

$$x = M \left/ \left(1 + \frac{g - 1}{2} M^2\right)^{1/2}\right.$$

Based on given conditions, the expected frequency of the cavity resonance can be compared to a measured power spectral density (PSD) calculations for accuracy. The PSD provides the magnitude of the resonance (in dB) at specific frequencies. In other words, PSD is a measure of how the power in a signal depends on frequency. The higher the PSD is at any given frequency, the greater the pressure fluctuations at the point where the pressure is measured, normally from a fast response pressure transducer.

Zhang and Edwards reported that for a given cavity dimension, a cavity of a given L/D produces a higher level of fluctuation for a Mach 1.5 freestream than for a Mach 2.5 freestream. They investigated a variety of length-to-depth ratios and found that a transition from a relatively weak transverse oscillation to a relatively strong

11

longitudinal oscillation occurs as L/D is increased from 1 to 3. Their data showed the standard deviation of the pressure normalized by the dynamic pressure of the freestream is a factor of three-to-four times higher for a Mach 1.5 freestream than for a Mach 2.5 freestream between L/D = 3 and L/D = 5. However, they do report the Mach 2.5 freestream leads to dominant modes (37).

Murray and Elliott utilized Schlieren photography and laser sheet lighting to study cavity flow for freestream conditions ranging from Mach 1.8 to Mach 3.5. Using the latter, they clearly illustrated the decreased coherence of spanwise flow structures as the freestream Mach number was increased from 1.8 to 3.5. They also report the convective velocity of the dominant structures was accurately estimated by 0.57 times the freestream velocity (16).

Unalmis et al. have reported results of a study of Mach 5 flow over a cavity for L/D=3 and L/D=7 using fast-response pressure transducers and laser sheet lighting. Interestingly, no evidence for coherent structures, typically induced by cavity acoustics at lower Mach numbers, was observed. Further, they reported substantially less coupling between the cavity pressure fluctuations and the shear-layer fluid dynamics as compared to similar flows with lower freestream Mach numbers. Lastly, they report that shock impingements on the trailing edge of the cavity are aperiodic for their conditions studied (34).

In a study of a cavity with L/D ranging from 4 to 7 and Mach numbers ranging from 0.8 to 3.0, Heller et al. (12) used a variable density wind tunnel to show the fluctuation level is very sensitive to the state of the incoming boundary layer in highly

compressible flow environments. They measured a normalized spectral peak nearly 30 dB higher for a laminar boundary layer, compared to a turbulent boundary layer, for a Mach 3 freestream. This was not the case for lower Mach number values where the state of the incoming boundary layer had little, if any, affect on the pressure spectra. The transition from a laminar to turbulent layer is a function of the Reynolds number. The Reynolds number (Re) is defined as (27:14):

$$\mathrm{Re} = \frac{Vd}{\boldsymbol{n}}$$

where V is the freestream velocity, d is the characteristic distance and ? is the kinematic viscosity. The critical Reynolds number for flow over a plate is $3.2\mathrm{x}10^5$, with lower values being laminar and greater values being turbulent (27:41). The characteristic distance most frequently used in cavity flow experiments is the direction of the flow between the upstream edges of the test section and the cavity. In each of these studies, a common theme is increased compressibility leads to reduce coherence of vortex structures as evidenced by both flow visualization and by direct pressure measurements.

Section 2 - Flow Control Basics

One application of flow control devices is to produce an environment more favorable to releasing stores. Although this experiment does not employ any type of flow control devices, it is noteworthy to mention other research that has. Flow control devices are either one of two types, passive or active, and are used to suppress the strong pressure fluctuations present in cavity flows. Passive approaches include the use of spoilers, cylindrical rods and stationary fences (30; 32; 33). Passive devices are designed to be extended into the incoming boundary layer to disrupt the formation of a coherent

spanwise shear layer and prevent the formation of cavity resonance phenomena. Passive devices are currently in use today on military aircraft.

Active approaches include the use of oscillating fences (26), upstream blowing (5; 9), and acoustic resonators (24; 32). All have been utilized to disrupt the evolution of well-organized spanwise vortical structures from the leading edge of the cavity. Oscillating fences are similar in design to stationary fences except they have a forcing function designed to oscillate the fence at a desired frequency. The desired oscillation frequency forces the shear layer at a frequency different from the cavity resonant frequency (25:94). Upstream blowing is the injection of air through a jet, usually immediately upstream of the leading edge of the cavity. The jets can operate continuously or they can be pulsed, although experimental results have shown that continuous injection is more effective than pulsed injection (5:7). Acoustic resonators can be low or high frequency relative to the predicted Rossiter modes with the newest research in high frequency areas. Experiments have shown high frequency resonators are able to reduce the resonance over all frequencies, not just specific frequencies as is the case with low frequency resonators (32:11). A recent comprehensive review of several types of flow control devices in a cavity flow environment is given by Cattafesta et. al. (6).

Section 3 - Store Motion Analysis

Flow in and around a weapons bay is approached from a different perspective by munitions experts concerned with the trajectory of a store as it is released. From this point of view, the highest priority is that the store separates cleanly from the aircraft and that its trajectory be predictable and controllable. In such an approach, the mixing layer is

often modeled as a steady flow region where the air velocity increases from a region within the cavity to the freestream (29:2). A time-dependent study of external store separation by Mosbarger and King lends credence to the general approach (15). However, given the resonant cavity phenomena, one might expect the fluctuations in flow properties to play a more prominent role in the free shear layer proximate to a cavity. Even minor variations in the store's initial trajectory could lead to unpredictability in the ultimate trajectory of the store. It is conceivable that acoustic suppression could improve the predictability of store trajectory.

To this end, varied approaches using computational fluid dynamics tools have been applied to cavity-store interaction problems. In 1992 Baysal et. al. published findings of a computational study utilizing a Reynolds averaging turbulence model to model a flow about a store-cavity combination where the store was placed alternatively within or wholly outside the cavity (2). In 1995 Maple and Belk developed the Beggar code, which offers the advantage of reduced user workload by automating the grid assembly process. Since the release of the Beggar code, it has been modified to meet evolving requirements and can now provide a fully time-accurate store separation prediction (4:2). More recently, Hamed et. al. utilized a high-order numerical method employing large eddy simulation to model the turbulence in a Mach 1.19 flow past a cavity with $L/D = 5$ (10:1).

Section 4 - Pressure Sensitive Paint Methodology

A typical PSP comprises two main parts: an oxygen-sensitive luminescent molecule placed within a transparent oxygen-permeable binder (3:159; 20). The PSP

method is based on the sensitivity of the luminescent molecules to the presence of oxygen. The luminescent material and the binder have evolved considerably since the creation of PSP. Early luminescent materials consisted of platinum octacthylporphyin, known as PtOEP using a silicone polymer as a binder. PtOEP had a pressure sensitivity of 0.72%/psig (meaning a 1 psig change in pressure will change the luminescence by 0.72% of the initial intensity) and a response time of 2.5 sec. (7:17). The newer PtTFPP (platinum tetra prophyin) using a FIB (flouroacrylic polymer binder) binder, there is a considerable improvement. PtTFPP has a pressure sensitivity of 6%/psig and a response time of 0.3 sec. (19). There are other formulas of PSP, but these two are mentioned here as a basis for comparing an evolving technology. In this study PSP provides only mean pressures, but as technology improves future work may include fluctuating pressures through the use of PSP.
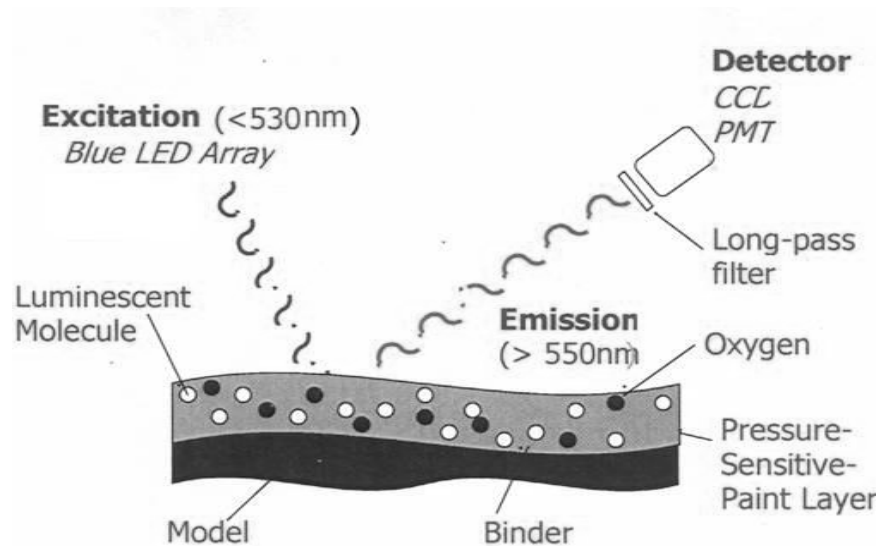
Figure 4. Simple schematic of PSP principle. (20)

Figure 4 shows a schematic of the PSP process. When a luminescent molecule absorbs a photon of a specific wavelength, it is excited to an increased energy state (excitation). The molecule then recovers to its initial state through the emission of a photon at a different known wavelength (emission) (20). In the materials used for PSP, oxygen collides with the molecules so the emission of the photon during the transition to the initial state is radiationless; this process is known as oxygen quenching. The rate of quenching is proportional to the local oxygen partial pressure, which is inversely proportional to the surface pressure. In other words, local regions with a higher rate of oxygen quenching display an increase in the intensity of light emission, which in air represents a lower local surface pressure (3:157). The emitted photons are collected through a charged-coupled device (CCD) camera after passing through a filter as shown. The governing equation for oxygen quenching is the Stern-Volmer Equation (13:17):

$$\frac{I_o}{I} = 1 + K_q P_{O2}$$

where I is the luminescence, I_o is the luminescence in a vacuum, K_q is the Stern-Volmer constant, and P_{O2} is the partial pressure of oxygen. I_o is frequently used as the intensity at atmospheric conditions since a vacuum is impossible to produce in most wind tunnels and in flight testing.

III. Experimental Set-up and Procedure

Section 1 - Wind Tunnel

The AFIT blowdown wind tunnel facility uses interchangeable convergent-divergent nozzles to generate variable speed flows. As shown in Figure 5, the wind tunnel is supplied with high pressure air (100 psi) which passes through a pressure regulator into the plenum chamber. The air then passes through a honeycomb flow straightener and through the nozzle, test section, diffuser and finally through large diameter piping into the vacuum tanks. Test runs of up to 20 seconds were possible, but most runs were on the order of 10 seconds.
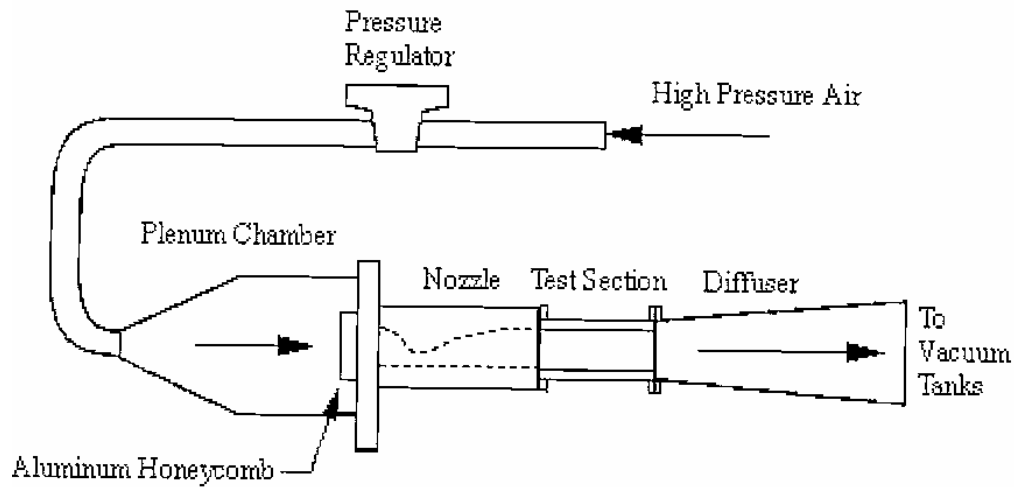
Figure 5. AFIT blowdown wind tunnel facility. Mach 2.9 nozzle shown (13:15).

The test section is 6.4 cm x 6.4 cm, excluding the cavity. Fast response pressure transducers (Endevco 8530C-50, 0-50 psia ± 0.5% and as noted Endevco 8530C-15, 0-15 psia ± 0.5%) were used to record the mean pressure in the plenum chamber and the mean pressure in the free stream of the test section. Complete specifications of the pressure transducers are found in Appendix C. The resulting pressure ratios yielded Mach numbers of 1.8 and 2.9 for the nozzles used. From this point forward, the nozzles will be referred to as Mach 1.8 or Mach 2.9. Flow properties for both nozzles are displayed in Table 1. Stagnation properties are from the plenum chamber, and freestream properties for the for test section. The Reynolds number is determined from the definition given in Chapter II.

Table 1. Flow properties for test conditions for the experiments.

	Mach 1.8	Mach 2.9
T_o	293 K (527 ^{o}R)	293 K (527 ^{o}R)
P_o	17.2 psi	26.8 psi
T_8	178 K (320 ^{o}R)	109 K (196 ^{o}R)
P_8	3.0 psi	0.80 psi
M_8	1.8	2.9
u_8	481 m/s (1580 ft/s)	606 m/s (1990 ft/s)
Re_x (est.)	5.7 x 10^5/m	4.6 x 10^5/m

Photos of the experimental set-up are shown in Figure 6. The cavity can be seen near the center of Figure 6(b) and the store is shown within its boundaries in Figure 6(c). For the remainder of the document, "clean" cavity refers to the cavity without the presence of the store. The pressure transducers are also visible in Figure 6(c). The transducers were flush mounted on the floor of the cavity for the reasons discussed in Chapter I. A pneumatic actuator mounted below the test section is able to thrust the store

from inside the cavity through the shear layer and into the supersonic freestream in 15 milliseconds. A bellows positioned about the rod was available to prevent ambient air from entering the test section through the cavity floor as is evident in Figure 6(a). However in most tests it was found that an o-ring seal about the support rod effectively sealed the tunnel.

(a)   (b)

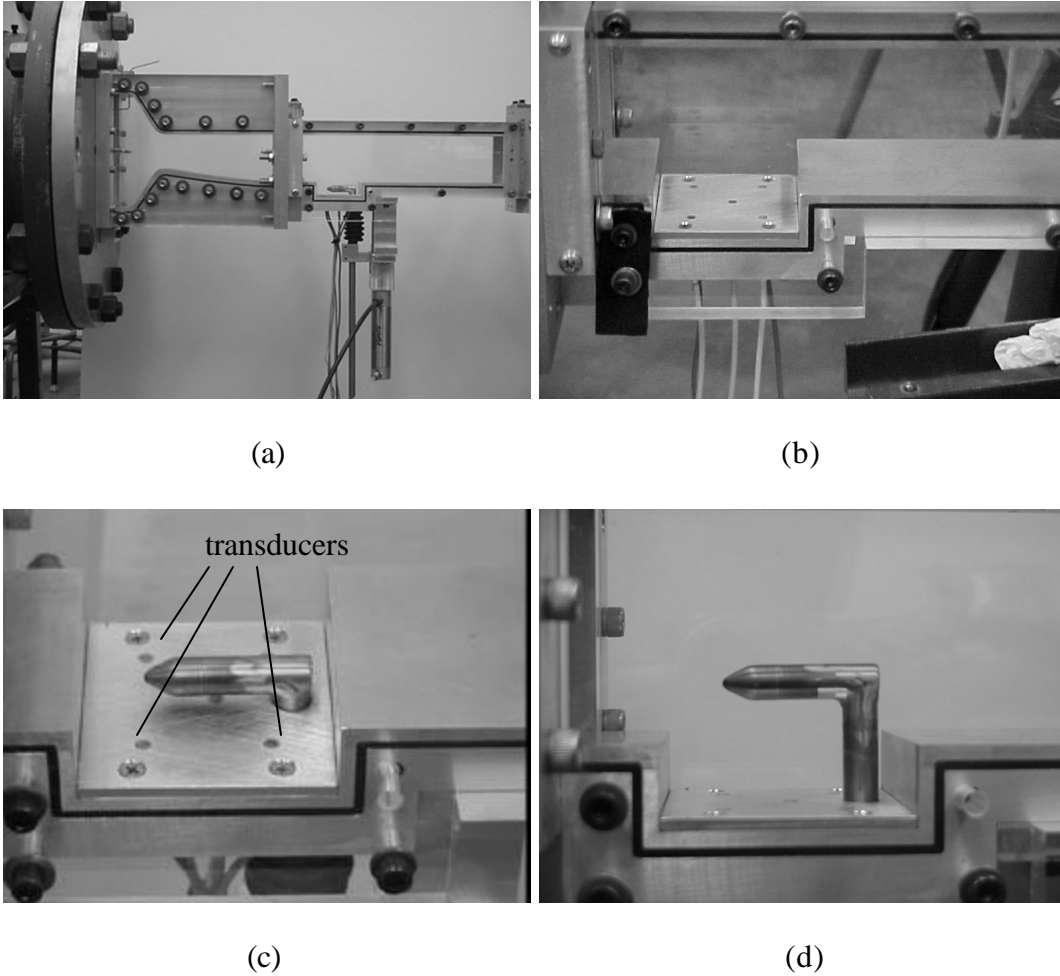(c)   (d)

Figure 6. Test section of the experimental apparatus: (a) Tunnel, Mach 1.8 nozzle and test section. (b) Clean cavity model with flush-mounted transducers present, (c) Cavity with the simulated store positioned within the cavity, and (d) Cavity with the simulated store extended into the freestream.

The cavity geometry is shown in Figure 7. The coordinate system used denotes x in the streamwise direction, y in the transverse, or vertical, direction, and z in the spanwise direction with $z = 0$ along the tunnel centerline. The cavity depth, D, was 1.7 cm, the cavity length, L, was 6.1 cm while its width, W was 6.4 cm and spanned the tunnel. The length to depth ratio (L/D) was thus 3.6 for each test performed. The store diameter, d, was 0.9 cm, and its length was 4.0 cm. Five transducers shown in Figure 7(b) are labeled #1: x = 1.5 cm, z = -1.7 cm, #2: x = 1.5 cm, z = 1.7 cm, #3: x = 3.3 cm, z = 0 cm, 34: x = 4.6 cm, z = -1.7 cm, and #5: x = 4.6 cm and z = 1.7 cm. Given the proximity of transducer #3 to the center of the cavity (x/L= 0.54 and z/W = 0), it is denoted the central transducer.

(a)   (b)
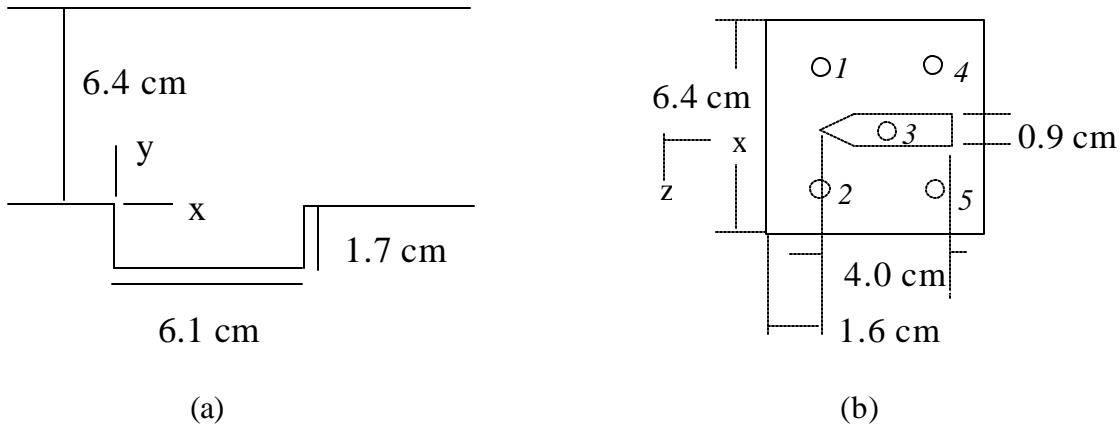
Figure 7. Schematic of (a) a side view of the cavity and (b) a top view of the store location within the cavity with approximate pressure transducer locations indicated with the small circles. Italicized reference numbers for the transducers are given in (b).

All transducers used were Endevco 8530C-50 (0-50 psig $\pm$ 0.5%) except where noted in Chapter IV. The transducers were connected directly to Endevco Model 4428A Conditioners and the data was acquired through a 1MHz Nicolet data acquisition system

to a PC. Pressure data was sampled at 100 kHz and roughly 65,000 data points were collected each run.

Section 2 - Pressure Sensitive Paint System

Pressure Sensitive Paint was applied to the floor of the cavity and to the simulated store as explained in Chapter I. The PSP used in this experimental procedure was Uni-FIB from Innovative Scientific Solutions Inc. (ISSI). Uni-FIB is a single layer PSP composed of a platinum tetra prophyin (PtTFPP) pressure-sensitive luminophore in a FIB binder. One of the key features of this type of paint is its insensitivity to temperature when utilized in combination with appropriate lighting and filters. PtTFPP has an excitation spectrum from 380 nm to 540 nm with a strong peak at 395 nm. The emission spectrum of PtTFPP is from 610 nm to 720 nm with a peak at 650 nm (19). For all testing conditions the PSP was illuminated by ISSI's 2 inch blue LED light source at 405 nm. The luminescence from the test area is captured by the camera after passing through a 610 nm Schott glass cutoff filter.

Images of the intensity of the PSP during various test conditions were taken with a 12-bit Photometrics HQ camera with a 1392 by 1040 imaging array. A single image was captured for each experimental condition. The typical exposure time was set differently for the two freestream Mach number conditions (approximately 0.2 seconds for Mach 1.8 freestream condition and 0.1 seconds for Mach 2.9) in order to take full advantage of the response time of the paint. In general, the mean pixel intensity recorded during an experiment was about 1500 while the dark image value was 90. Care was taken to prevent saturation of the camera (pixel intensity of 4096) anywhere within the field of view. Figure 8 is representative of the range of intensities present at different pressures,

22

as shown by the linear and non-linear regions. For pressures ranging from 2 to 5 psi, a 0.1 psi change in pressure resulted in a change of 15 pixel levels of intensity. For the non-linear region, from 0 to 2 psi, a 0.1 psi change in pressure resulted in a change of approximately 71 pixel levels.
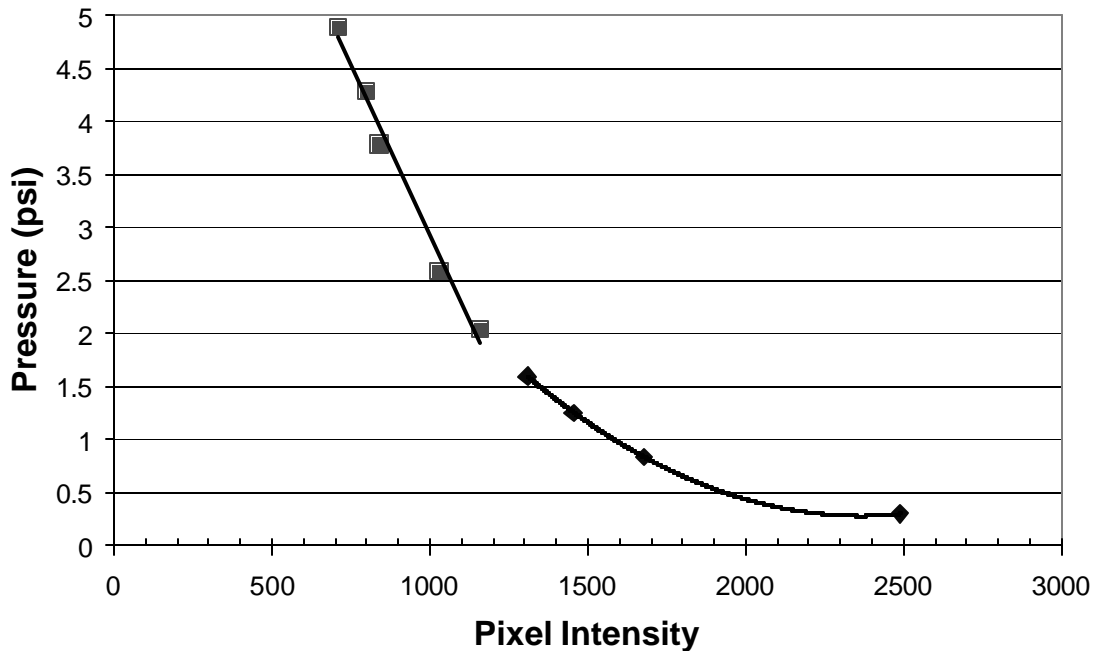
Figure 8. Pixel intensity response to pressure change.

On days when PSP data was being taken, the experimental procedure began with an in-situ calibration of the PSP. Since the AFIT blowdown wind tunnel facility is capable of generating a variety of mean pressures in the test section based on residual pressure within the vacuum tank, the in-situ calibration was straight forward. A minimum of eight pressure levels were utilized during calibration. The calibration coefficients (or Stern-Volmer coefficients) were determined by processing the known pressure values

along with their corresponding images through ISSI's calibration software. When calibration of the PSP on the store was required it was placed at the y = -1 cm position. In this situation the pressure transducers were not directly on the surface, such as when the PSP on the cavity floor was calibrated, but they were in close enough proximity to accurately calibrate the PSP. The calibration software can essentially fit a ninth order polynomial in the form of (3:184):

$$p = c_0 + c_1\left(\frac{I_{ref}}{I}\right) + c_2\left(\frac{I_{ref}}{I}\right)^2 + c_3\left(\frac{I_{ref}}{I}\right)^3 + \ldots\ldots\ldots$$

For this experiment a second order polynomial (only three coefficients) was sufficient to calibrate the paint since temperature effects were negligible in the temperature range of the tests. Despite the fact the calibration software automatically produced the calibration coefficients, a sample calibration curve along with the subsequent polynomial is shown in Figure 9. The daily calibration procedure was necessary in order to account for changes in the luminescence properties of the PSP over time.

$$p = -0.9133 + 5.4383(I_{ref}/I) + 8.0244(I_{ref}/I)^2$$
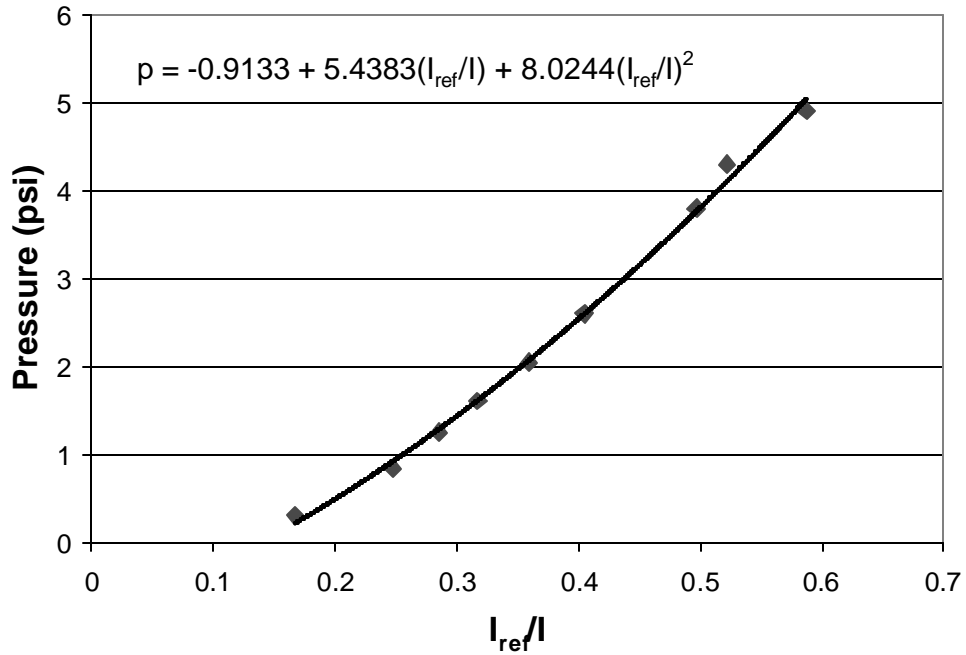
Figure 9. Sample calibration curve for Mach 2.9 freestream flow.

For image processing purposes a reference image was acquired at ambient pressures, known as a "wind-off" image. In addition, a "dark" image (PSP lighting system off) was taken to characterize the ambient light in the room. These two images along with the images acquired during testing conditions, or "wind-on" images, were processed to obtain surface pressure contours using ISSI's Pro-Image spatial mapping software. Using the corresponding calibration coefficients and the "dark", "wind-off", and "wind-on" images in ISSI's Pro-Image Software, the mean pressure over the painted surface, whether it was the cavity floor or the simulated store, was determined. To verify the accuracy of the calibration, the mean pressure measured by the PSP was then compared to the mean pressure measured by the transducers, bearing in mind the PSP values are from the pixel location nearest the transducer since the transducers themselves

were not painted. Results are shown in Table 2. For a more thorough discussion of the measurement technique, the reader is referred to Bell et.al. (3).

Table 2. Correlation of Transducer and PSP pressure readings. Data from Mach 1.8 (freestream) with no store present.

| Transducer | Pressure (psia) | | % |
Number	Transducer	PSP	Difference
1	4.18	4.23	1.18
2	4.26	4.25	-0.24
3	4.03	4.04	0.02
4	3.99	4.02	0.59
5	3.94	3.99	0.97

The PSP data collection occurred in several steps. The cavity floor mean pressure data was obtained either without the store present or using an un-painted store with the PSP applied to the cavity floor. The components were painted (and therefore tested) separately for the main reason the camera lens could not focus on both the cavity floor and the store at the same time. When the un-painted store placed within the cavity it was manually positioned at four different heights with respect to the cavity edge (y = 0). Positions were below the edge (inside the cavity) at y = -1 cm and y = -0.5 cm. Positions above the cavity (freestream) included y = 0.5 cm. All intensity images were taken directly above the cavity using the Photometrics camera.

When the painted store was used the cavity floor was unpainted. In addition to the previous four positions used, two more positions were added at y = -0.25 cm and y = 0.25 cm due to the high variability of the pressure on the store in this range. Intensity images were taken with the camera positioned directly above and also at a position of roughly 45

degrees off the nose of the store and slightly below the store. The same procedure and conditions were used for both the Mach 1.8 nozzle and the Mach 2.9 nozzle.

Section 3 - Schlieren Photography
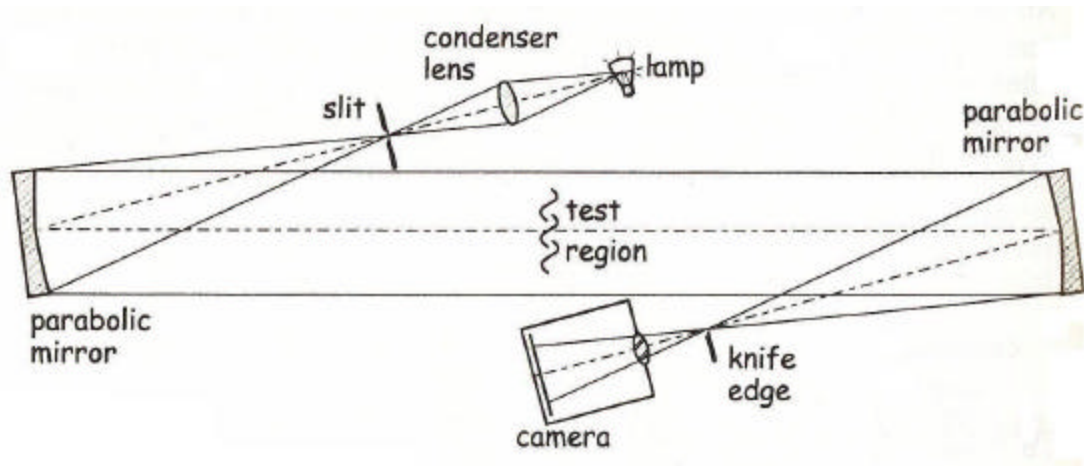
Figure 10. Schlieren photography set-up (28:42)

The standard Z set-up was used for the high speed Schlieren photography, as shown in Figure 10. The parabolic mirrors were 12 inches in diameter and had a focal length of 80 inches. The light source was a continuous wave high DC voltage mercury arc lamp with an intensity of 140,000 candles per square centimeter. The images were taken at either 4,000 frames per second or at the equipment maximum speed of 16,000 frames per second with a shutter speed of 1/128,000 using a Photron FASTCAM-X 1280 PCI camera manufactured by Cooke. The knife edge was placed in the horizontal position, with the edge positioned on top. At 4,000 frames per second, the entire test section above the cavity was visible, making it ideal for visualizing the interaction of the cavity and the freestream. At 16,000 frames per second the images were smaller and

27

focused on the structure of the shear layer that formed over the cavity at the various test conditions. Images were processed through a PC using Photron Motion Tools software program. Real-time variations in the Schlieren images due to rapidly changing density field were captured. Schlieren images were obtained after all PSP data was collected due to the extensive set-up of both data acquisition systems.

IV. Results

Section 1 - Clean Cavity

To begin to understand the interaction of the cavity and the simulated store, the initial step is to begin to characterize the flow field for the clean cavity without the store present. This baseline information is instrumental to determining the effect of the store on the cavity system.

Section 1.1 - Pressure Sensitive Paint Data

Initial PSP measurements were performed on the cavity floor. The global mapping of the mean pressure and the pressure coefficient, following the convention of reference 31, for the cavity floor at free stream Mach numbers of 1.8 and 2.9 are shown in Figure 11. For the Mach 1.8 case, the pressure along the span of the farthest downstream portion of the floor is roughly 39% higher than that of the upstream portion of the floor. One interesting characteristic of the Mach 1.8 case is the "u" shaped region of lower pressure present upstream of the pressure rise at the trailing edge of the cavity, which indicates a three-dimensional circulation pattern in the region. This phenomenon is not clearly identifiable in the Mach 2.9 flow. Overall, the pressure map appears more uniform for the Mach 2.9 freestream. These results are generally consistent with the findings of reference 31, where static pressure measurements were taken along the spanwise center of cavities for a variety of geometries and flow conditions.
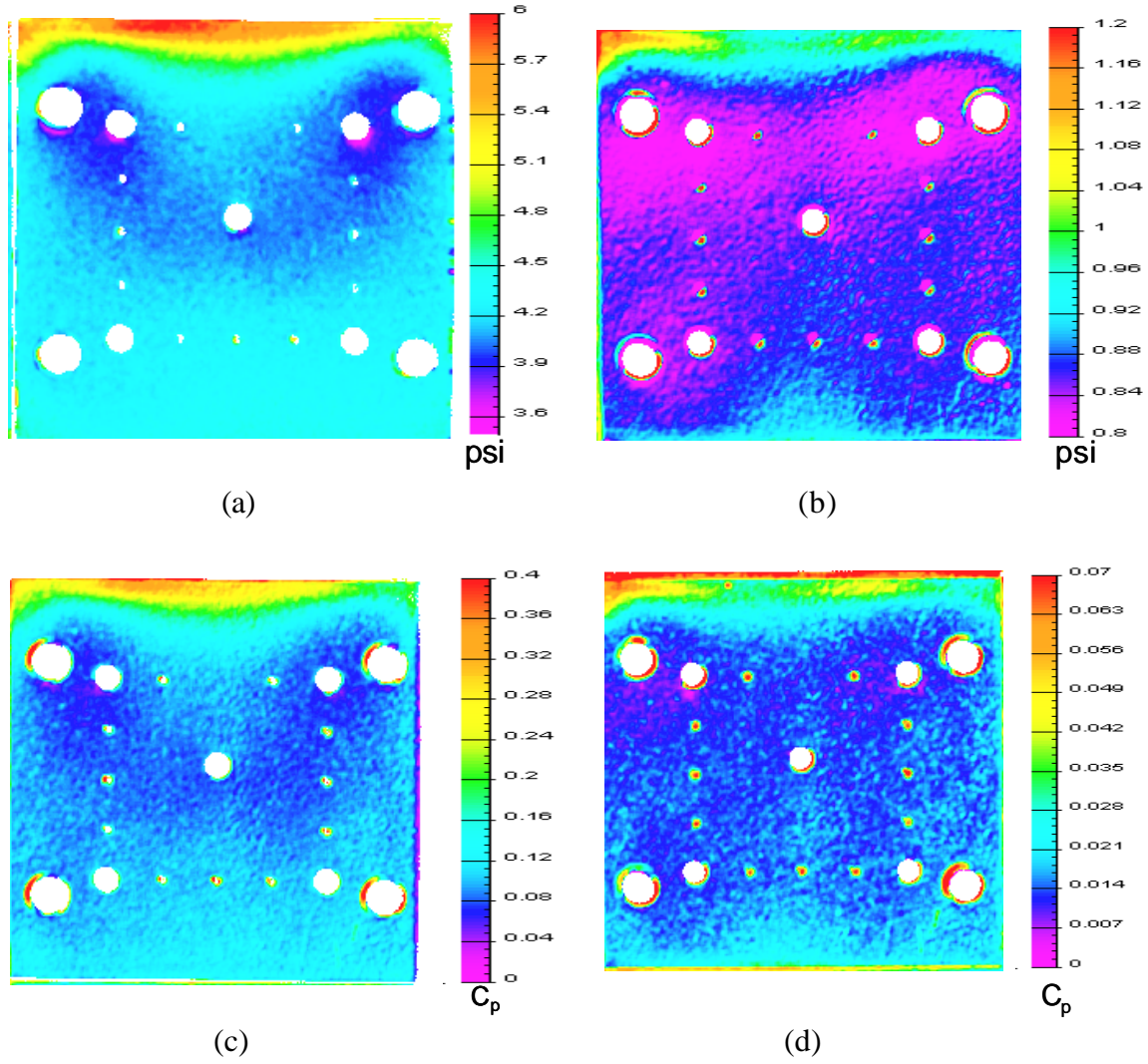
Figure 11. PSP measurements of cavity floor with no store present. (a) Mach 1.8 mean pressure, (b) Mach 2.9 mean pressure, (c) Mach 1.8 C_p, (d) Mach 2.9 C_p. Flow direction is from bottom to top.

As a comparison to existing data, the pressure coefficient calculated from the PSP data was compared to similar data from NASA Technical Paper 2683 (31:12). The existing data is for L/D = 4 and W/D = 5 whereas the data from this experiment is for L/D = 3.6 and W/D = 3.8. The PSP data is obtained slightly offset from the centerline since pressure transducer #3 was located on the centerline, while the NASA data is from

the centerline. Considering these minor differences in cavity geometry results are consistent with the expected open cavity behavior. There is a slight difference at the trailing edge as shown by the higher C_p for the larger L/D cavity in Figure 12. This is expected from the discussion in Chapter II and Figure 3 as the cavity moves closer to the geometry associated with closed cavity flow.
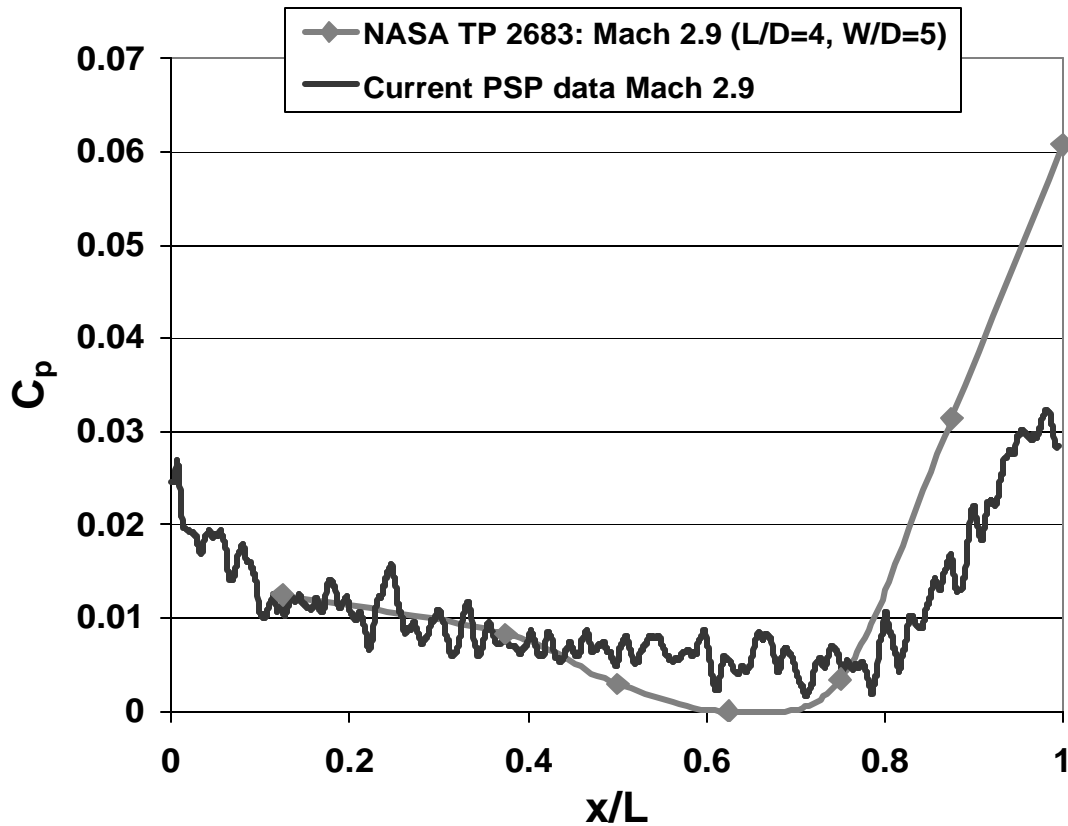
Figure 12. Comparison of C_p results to existing data as a function of streamwise distance.

Section 1.2 - High Speed Pressure Transducer Data

Pressure data was acquired by each Endevco transducer at 100 kHz. To verify the correlation of the PSP pressure data to the pressure transducers a single plane of PSP data

adjacent to transducers #1 and #4 was compared to the mean pressure of transducers #1

and #4. The results are shown in Figures 13 and 14. Error bars for the combined ±0.5%

error (0.50 psia) of the transducers along with the signal conditioners are included in the

figures.
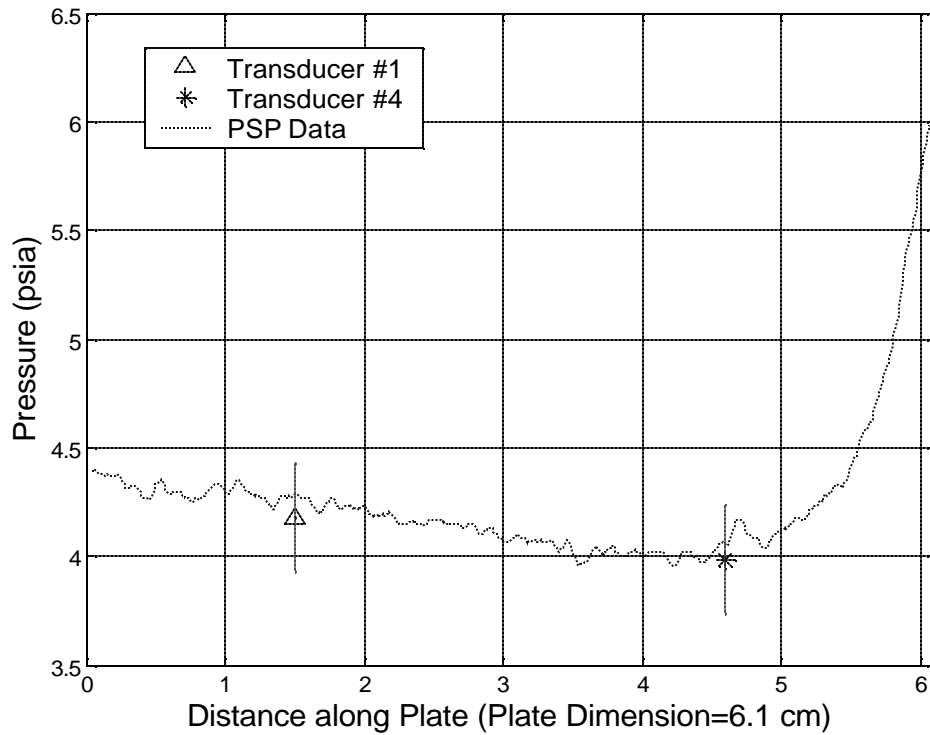
Figure 13. PSP Data correlation to pressure transducer data for Mach 1.8.
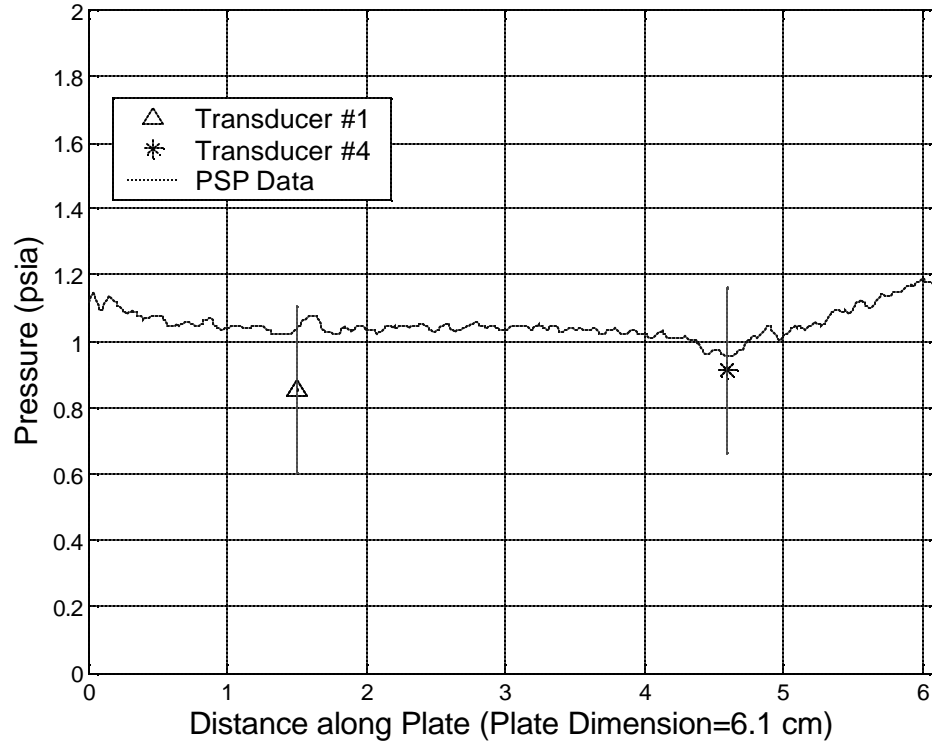
Figure 14. PSP Data correlation to pressure transducer data for Mach 2.9.

The high-speed transducers were used to analyze the fluctuation of the pressure on the cavity floor to further understand the clean cavity flow field. The pressure transducer data was grouped in bins of 512 points and 196,608 data points were used to calculate the power spectra plots. A plot of temporal pressure fluctuations normalized by the mean pressure is shown in Figure 15 for the central transducer (#3) with no store present for Mach 1.8 and Mach 2.9 test conditions. The corresponding power spectra are given in Figure 16.
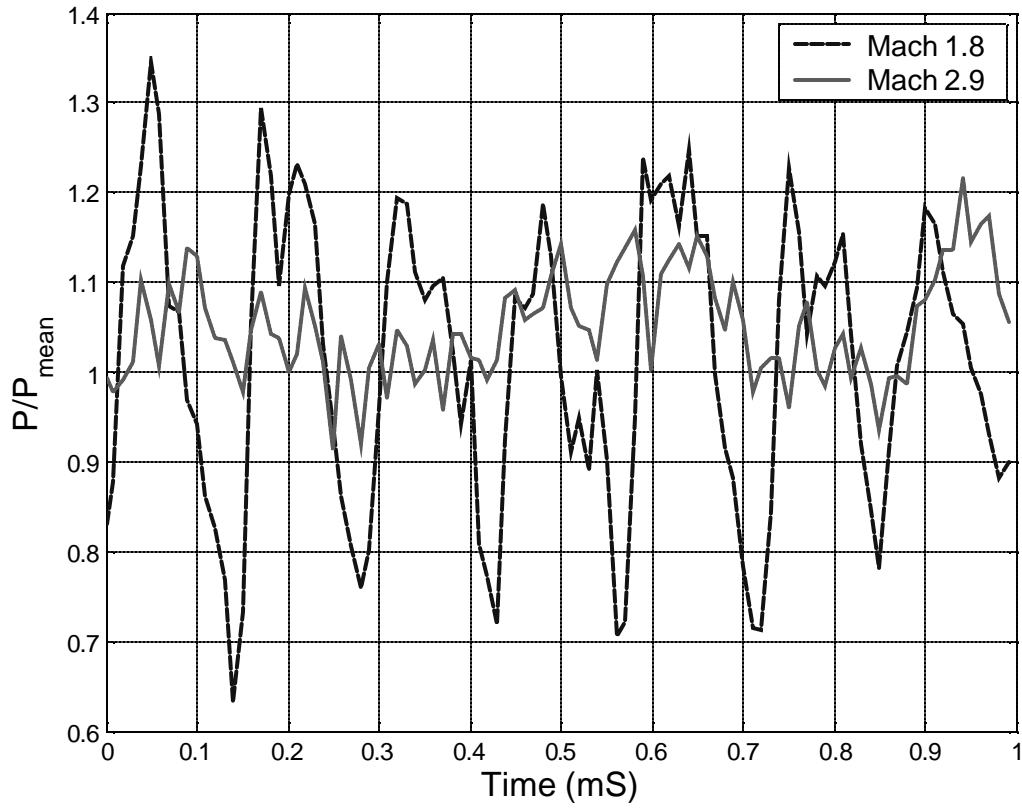
Figure 15. Normalized temporal pressure data for Mach 1.8 and Mach 2.9 for the central transducer. No store is present.
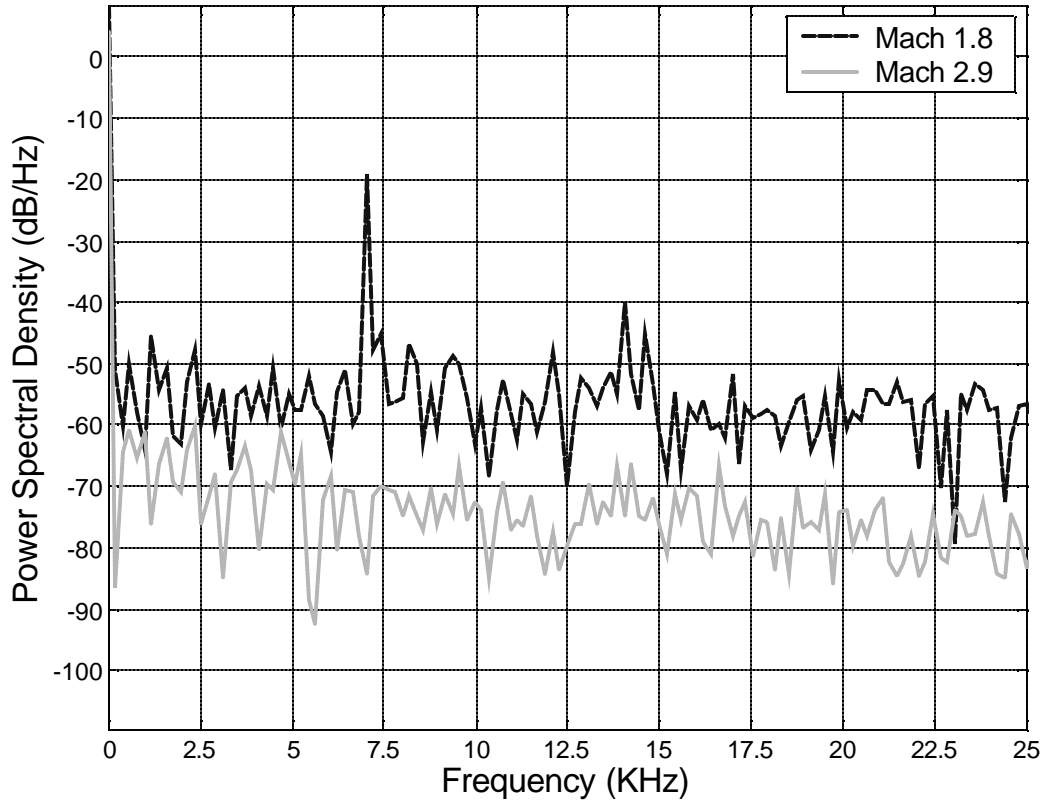
Figure 16. Frequency spectra from the pressure measurements taken from the central transducer (#3) located within cavity floor. No store is present.

The Mach 1.8 condition yielded a strong peak near 7 kHz with a weaker sub-harmonic peak located near 14 kHz. Using the approach of Rockwell and Naudascher, the $n = 5$ Rossiter mode under the test conditions equates to a frequency of 7.0 kHz. For one point of comparison, Zhang and Edwards report dominant mode peaks at roughly 6 kHz at Mach 1.5 in a cavity with an L/D of 4.0 (37:361).

Figure 16 also displays the absence of a distinct peak in the spectra taken from the cavity floor for a free stream Mach number of 2.9. This result was in stark contrast to the Mach 1.8 results. In order to rule out the possibility the lower mean pressure values

35

corresponding to the Mach 2.9 freestream were responsible for the lack of a measured coherent spectral peak, the 50 psia Endevco transducers in locations #3 and #4 were replaced with 15 psia transducers, thereby increasing the signal-to-noise ratio by a factor of three. The differences between the data collected by the transducers can be found in Appendix B. While the 15 psia transducers did exhibit a higher standard deviation, which correlates to greater pressure fluctuations, the spectral data for each location did not change appreciably and the 50 psia transducers were reinserted and used for the remainder of the experiment. Rossiter concluded that at transonic speeds, flow over a cavity contains periodic and random components, with the random component dominating for a L/D > 4 and the periodic component dominating for a L/D < 4 (23:12). This is consistent for the Mach 1.8 freestream case, but more investigation is required for the Mach 2.9 freestream condition.

As noted in Chapter II, Heller et al. showed the upstream boundary layer state influences the development of cavity tones for a Mach 3 freestream but was of less consequence for lower freestream Mach number values (12:548). The Reynolds Number (Re) was calculated to be $4x10^5$ for the Mach 2.9 freestream and $6x10^5$ for the Mach 1.8 freestream, both values generally corresponding to a turbulent boundary layer over a flat plate. While the incoming boundary layers are both classified as turbulent, the frequency spectra display very different results, but consistent with the findings by Heller et. al.

Section 1.3 - Schlieren Photography Data

Averaged Schlieren images were obtained with an exposure time of 0.001 seconds and provided a good visualization of the overall flow structures in the proximity of the cavity. In Figure 17, the flow is moving left to right for each case and both freestream

Mach numbers exhibit similar features. Both images have the characteristic leading and trailing edge shocks usually associated with open cavity flows and each contains a region of sharp contrast along the free shear layer. The obvious difference is the angle of the shocks with respect to the horizontal. In the Mach 2.9 freestream case the shocks are canted over more, or more attached than at the lower Mach number, which is consistent with compressible flow theory. Some other items to mention are the superfluous shocks emanating from the upper left side of the images. These are due to discontinuities in the transition from the nozzle to the test section. At the time these images were recorded there was also a scratch on the wall of the test section in the images within the cavity that is visible.
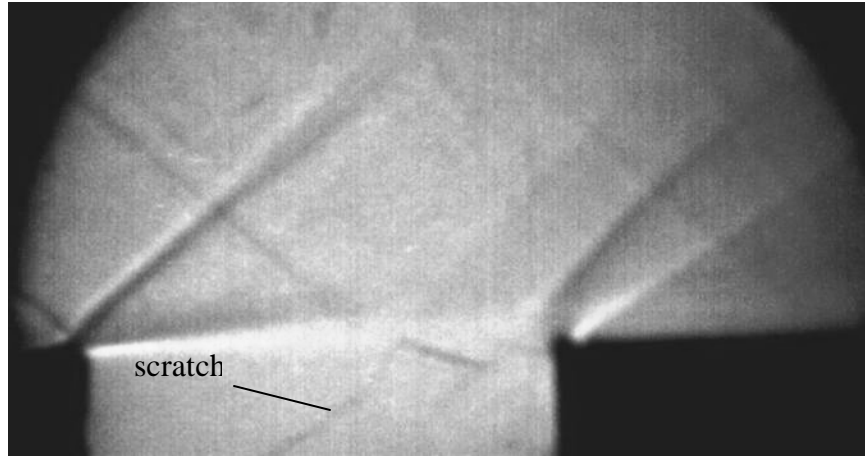
(a)
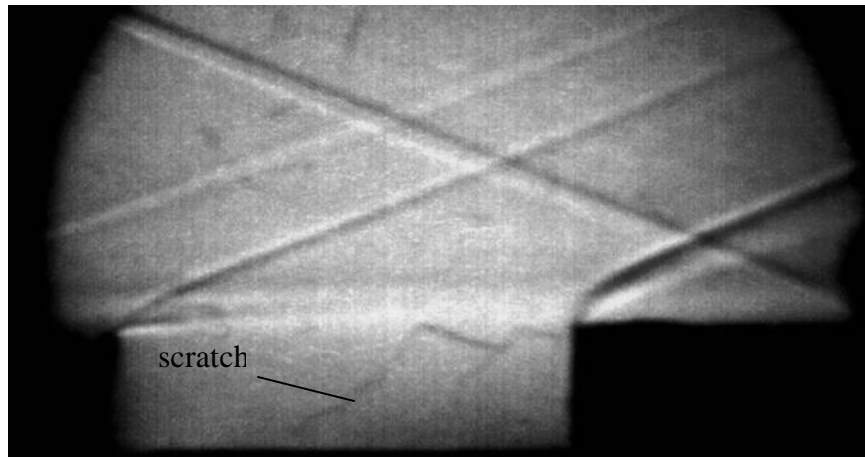
(b)

Figure 17. Averaged Schlieren photography of cavity taken with an exposure time of 0.001 seconds without store present. Flow is from left to right. (a) Mach 1.8, (b) Mach 2.9.

To characterize the time-dependent properties of the free shear layer sequences of successive Schlieren images of the clean cavity were collected and analyzed. The images were acquired at 16,000 frames per second with a shutter speed of 1 microsecond. In the Mach 1.8 flow, views of the classic "whipping" flow and widening shear layer that are commonly associated with flow over a cavity were captured. A sample is shown in

Figure 18. Additional images are found in Appendix A. Using the average convective velocity within the shear layer ($U_c=0.57U_8$) confirmed by Murray and Elliott (16:846), one would expect a structure to convect 1.7 cm (0.68 inches, which is 0.28L) downstream per frame. This corresponds well qualitatively to the results shown in Figure 18, where a single structure is subjectively tracked from approximately 0.2L to 0.8L in the course of three successive frames, as noted by the arrows.

Figure 18. Five successive Schlieren images separated by 6.25e-5 seconds characterizing the shear layer for Mach 1.8 flow. Flow is from left to right.

When the Mach number was increased to 2.9, the "whipping" motion clearly identified for Mach 1.8 was not present. The most likely explanation is the structures within the free shear layer decrease in spanwise coherence, or become more three-

dimensional. As a result, the optical averaging inherent to Schlieren photography conceals the convection and development of individual density waves. Because of this, it became nearly impossible to qualitatively correlate flow structures from frame-to-frame in any meaningful way, as can be seen in Figure 19. Additional images are found in Appendix A. The arrows are a subjective attempt to follow a singe flow structure downstream. While the freestream velocity was somewhat higher, the predicted downstream movement of a single flow structure is 2.2 cm (0.85 inches, which is 0.35L) per frame which falls within the range that could be captured by the camera in real time. That being said, there are some interesting features of Figure 19 which should be noted. For example, an individual shock emanating from a particularly strong flow structure within the shear layer is evident in the third image.
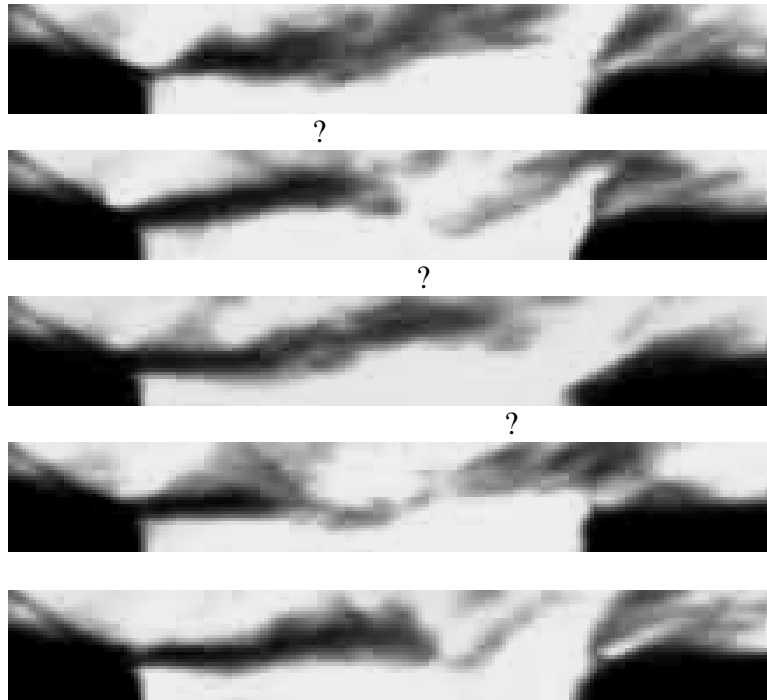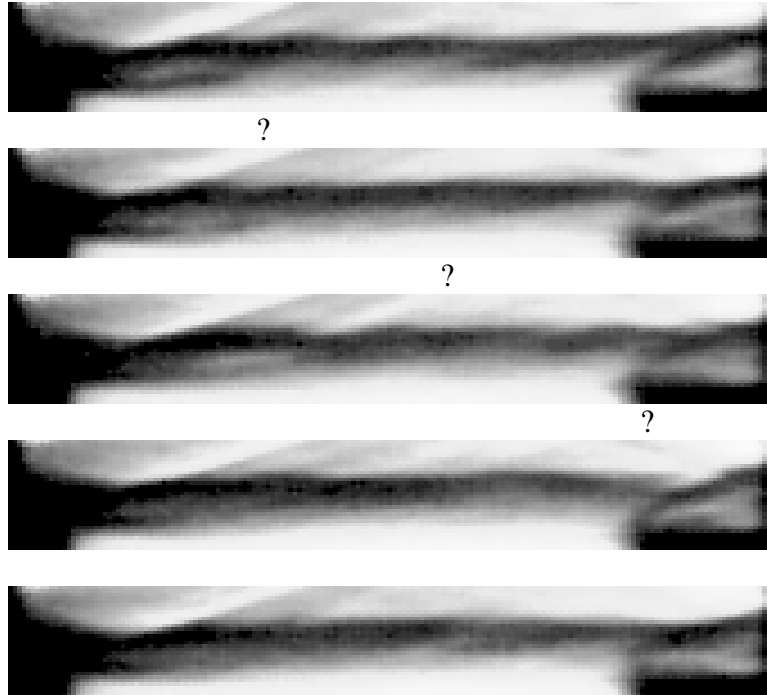
Figure 19. Five successive Schlieren images separated by 6.25e-5 seconds characterizing the shear layer for Mach 2.9 flow. Flow is from left to right.

Section 2 - Cavity with Store Present

To study the interaction of the cavity and store system, two approaches were taken. To begin, the store was placed at several different stationary heights. Pressure transducer data on the cavity floor, PSP data on the cavity floor and the store itself, and Schlieren photography were all employed to characterize the flow field. Second, Schlieren photography was used to examine the effect of the system as the store was thrust from inside the cavity through the shear layer and into the freestream.

Section 2.1 - Cavity with Stationary Store Present

Section 2.1.1 - High Speed Pressure Transducer Data

To begin with, the effect of the presence of the store on the frequency spectra is examined. Figure 20 displays the frequency spectra measured by the central transducer (transducer #3) for the Mach 1.8 freestream flow. As the store placement was changed from inside the cavity to locations nearer to, and finally within the free stream, the magnitude of the resonant peak diminished. With the store positioned within the cavity, the spectrum is qualitatively similar to that of the cavity without the store present. There is a peak at 7.0 kHz, though its amplitude has been reduced by about 17 dB, compared to the clean cavity. Likewise, a sub-harmonic is present at 14 kHz. With the store positioned at $y = -0.5$ cm, the peak in the spectra shifted from 7.0 kHz to 6.8 kHz and increased slightly while the level of the sub-harmonic dropped slightly. With the store position increased to $y = 0$, the peak frequency shifted downward to 6.6 kHz, and the level dropped slightly. With the store positioned at $y = 0.5$ cm the tone dissipated to the level where it was undetectable from background noise, with similar results at $y = 0.8$ cm. The general trend is the periodic pressure fluctuations diminish as the store moves from inside the cavity through the shear layer and into the free steam. Analysis of the Mach 2.9 frequency spectra for various store positions yielded similar results to the clean cavity conditions shown in Figure 16 in that no clearly identifiable resonant peaks were observed.
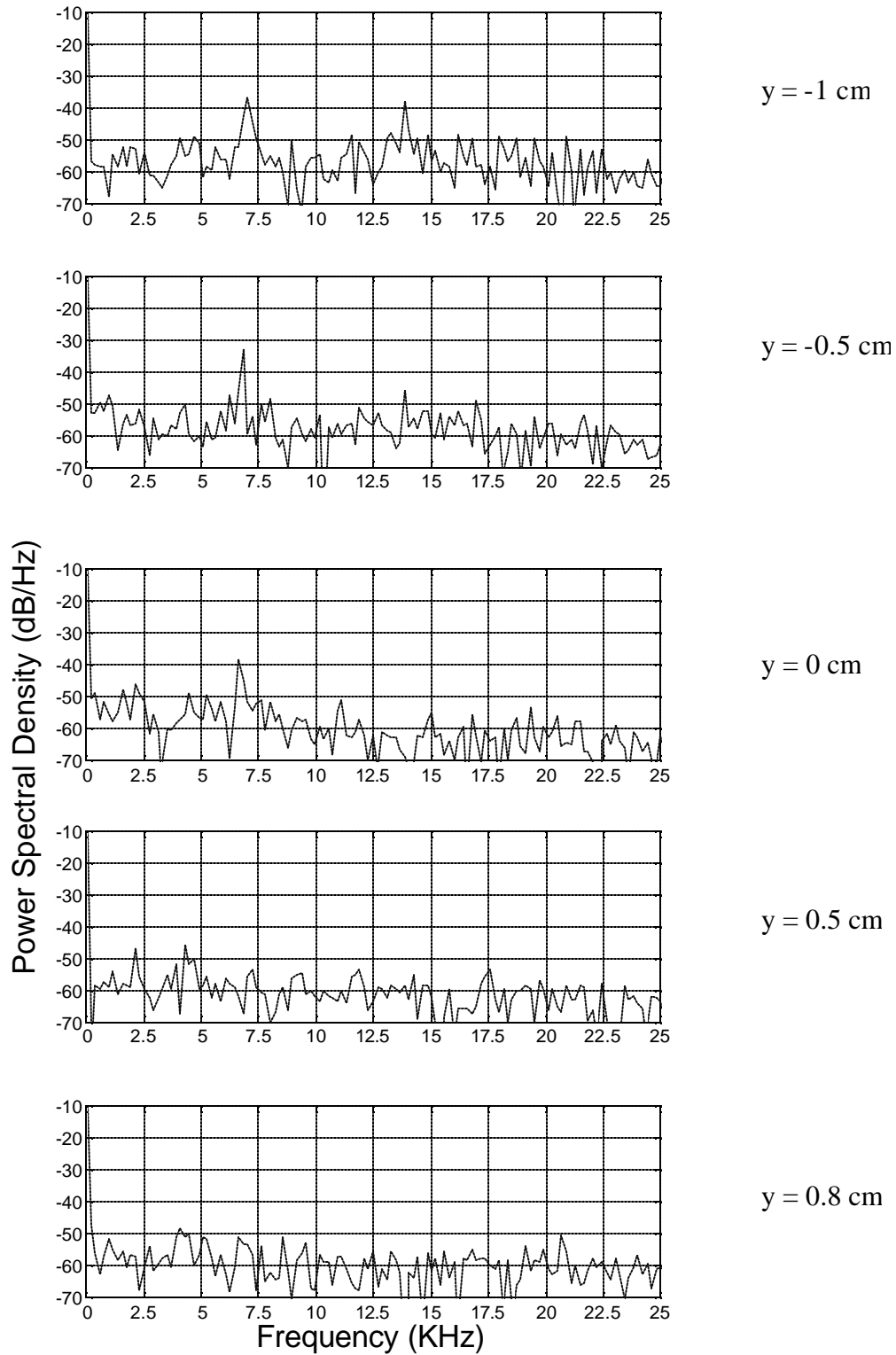
Figure 20. Frequency spectra taken from the central transducer for a stationary store at 5 different vertical positions for free stream Mach number of 1.8.

To analyze at the pressure fluctuations from another perspective, the standard deviation of the pressures of the central transducer (transducer #3) and transducer #4, located near the rear wall of the cavity, for both free stream Mach numbers at various store heights is examined. In Figure 21, the standard deviation of the pressures is normalized by their respective free stream pressure and the effect of store location on this value is plotted. The first noteworthy difference is the overall trend of the Mach 1.8 versus the Mach 2.9 cases. The central transducer for the Mach 1.8 condition revealed an overall decrease in the standard deviation as the store was moved from inside the cavity into the free steam while transducer #4 was nearly constant. This is consistent with the frequency spectra data from the central transducer shown in Figure 20 that shows a decrease in the resonant peaks as the store moves into the freestream. Interestingly, the Mach 2.9 case has the opposite trend as the standard deviation of the pressure increases as the store is extended into the free stream. No comparisons can be made with the frequency spectra data since a resonant peak was not seen at any store location for the Mach 2.9 condition. However, it does reveal the influence the store has on the fluctuation of the pressure on the cavity floor.

One possible explanation is that as the store is moved into the Mach 2.9 free stream, it may divert more energy from the supersonic flow into the shear layer and subsequently into subsonic cavity region, generating greater pressure fluctuations. By contrast, the energy in the Mach 1.8 freestream is likely introduced by the "whipping" motion. In this flow the store apparently disrupts the coherence of the shear layer, reducing the "whipping" motion and subsequently reducing the measured level of

pressure fluctuations. The increased level of fluctuations for the Mach 2.9 case is particularly pronounced for transducer #4, located closer to the rear wall.
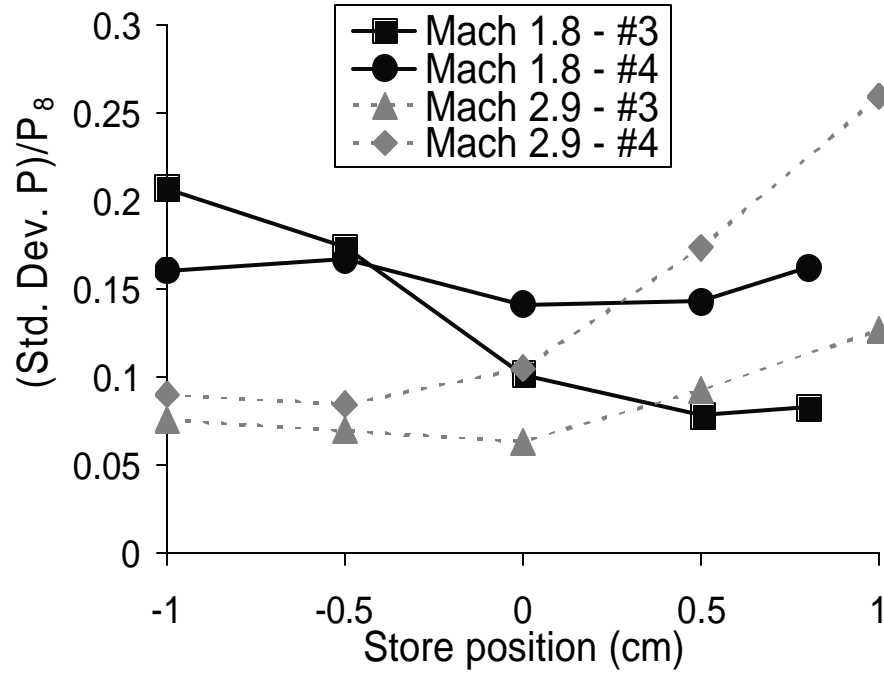
Figure 21. Standard Deviation of pressure from central transducer and transducer near trailing edge of cavity as a function of store location for Mach = 1.8 and Mach = 2.9. The y = 0 location is along the plane of the cavity lip.

Regardless of the veracity of this hypothesis, Figure 21 raises some significant concerns. First of all, different speeds have a different effect on the flow conditions within the cavity as the store moves through the shear layer. It appears at lower supersonic speeds the store attenuates the cavity resonance, but when the Mach number is increased, the fluctuations tend to increase when the store is positioned in the shear layer. The second concern is the increase in the pressure fluctuations closer to the rear of the

cavity. This becomes a concern in weapons bays where stores are placed head to tail, the stores located at the rear of the weapons bay are subjected substantially to different release characteristics than at the front of the weapons bay. This configuration is mostly used with "dumb" bombs that have no means of correcting an undesired release trajectory. Therefore the probability of one or several of the stores missing their intended target is increased. Another problem is weapons at the rear of the cavity are subjected to these higher fluctuations which can lead to frequencies that coincide with the natural frequency of the tail assembly of the store. This leads to significant damage, and obviously, an unusable weapon.

Section 2.1.2 - Schlieren Photography Data

A time-averaged Schlieren visualization of the cavity with the store present is given in Figure 22 and is compared to Figure 17 to determine the effect of the presence of the store. The images were acquired with an exposure time of 1 millisecond. With the store positioned completely within the cavity there is no visual effect from the store on the creation of the shear layer as the flow interacts with the cavity. It must be noted the images were obtained at different times and subtle differences in lighting between the Mach 1.8 and Mach 2.9 are due to small variations in the set-up of the Schlieren equipment. Notable features of the unimpeded flow are the shock wave at the leading edge, the free shear layer, and the shock impinging upon the downstream portion of the cavity. It also appears that an oblique shock is located just downstream of the cavity. The observation of these components of the flow field is consistent with published results.
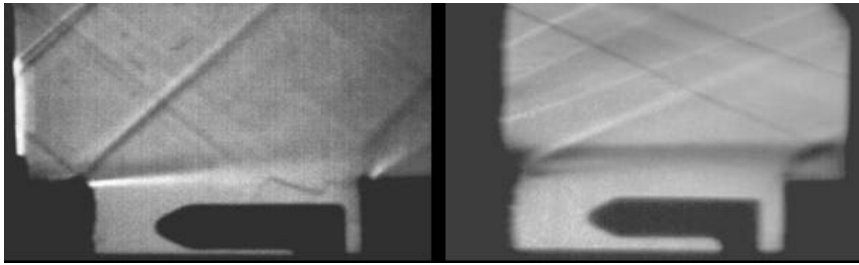
y = -1 cm
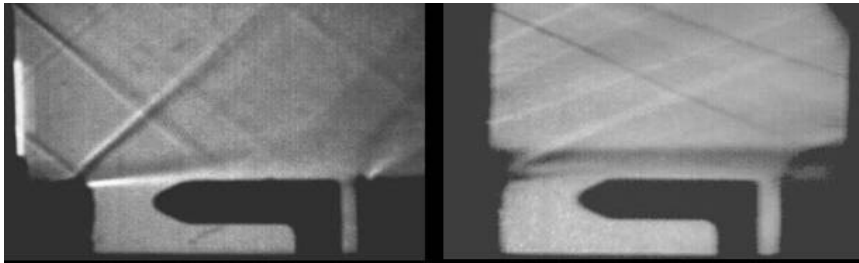
y = -0.5 cm
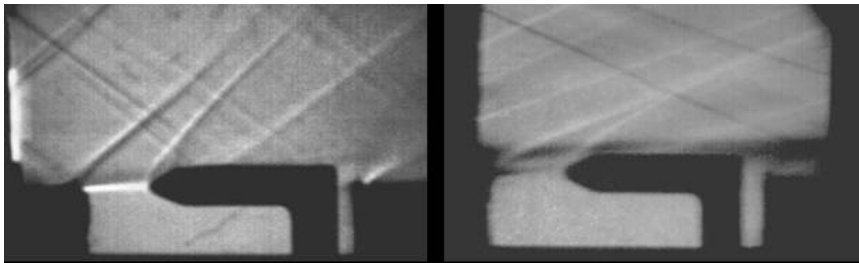
y = 0 cm
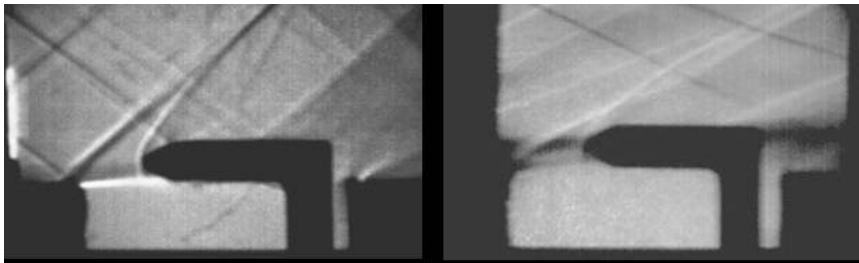
y = 0.5 cm
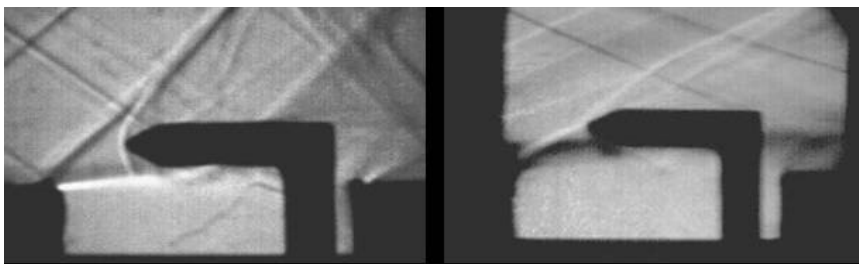
y = 1 cm

Figure 22. Schlieren of the flow with a stationary store at five locations in the shear layer as noted. Left column is Mach 1.8, and the right column is Mach 2.9. Exposure time was 0.001 seconds. Flow is from left to right.

As the store begins to enter the shear layer at the $y = 0$ position, the store dramatically changes the flow properties. The most obvious change is the shock wave that forms on the nose of the store as it enters the supersonic flow. A small expansion fan is attached to the store's upper surface as the conical nose transitions to the cylindrical body. One difference visible between the Mach 1.8 and Mach 2.9 case is the impingement shock on the rear of the cavity is disrupted in the Mach 2.9 flow, but is still visible in the Mach 1.8 flow.

At store position $y = 0.5$ cm the nose of the store is slightly above the free shear layer and a shock wave appears to be forming on the underside of the store toward the cavity as well as continuing into the free steam. In comparison with the clean cavity images, there is evidence the store is "pulling" the shear layer away from the top of the cavity as the store moves through the shear layer. This phenomenon is further explored later in the document when the moving store is analyzed. The impingement shock is still visible for Mach 1.8 but not Mach 2.9.

The small difference in the location indicated for the last row of images arises because when the store was positioned at $y = 1.0$ cm in the Mach 1.8 flow, the flow was choked at the store location. This was not an issue for the Mach 2.9 condition and thus the $y = 1.0$ position was used. At this y-location the store has exited the cavity, except for the attachment rod. Notably, the shock ends when it hits the shear layer at the cavity. One would expect an expansion fan to be reflected back toward the store. Indeed, upon close observation, a subtle pattern can be identified for freestream Mach numbers of both 1.8 and 2.9. However, this property is difficult to see clearly, in part because of the spanwise optical averaging inherent to Schlieren photography.

The upstream portion of the shear layer appears to continue to shift toward the store. However, in the images corresponding to Mach 2.9 the impingement shock on the trailing edge is clearer and comparable to the images corresponding to the store placement within the cavity, despite the presence of the attachment rod. The strong density gradients responsible for the bright and dark regions of the picture suggest that a released store undergoes great variations of pressure between its upper and lower surfaces as it moves out of the cavity into a supersonic freestream. This is corroborated by the literature and by analysis of the PSP data.

Section 2.1.3 - Pressure Sensitive Paint Data

PSP data was acquired on the cavity floor with a store fixed in place for each Mach number and is shown in Figure 23. The mean pressure on the cavity floor with the store in place displays a similar pattern as those taken without the store with the exception of a slight overall increase in mean pressure. As the store is moved out of the cavity the mean pressure continues to increase. At position of $x = 5$ cm and $z = 1.3$ cm the pressures were compared for the various store heights. For the Mach 1.8 freestream the pressure increased from 4.3 psi to 5.3 psi, roughly a 25% increase. For the Mach 2.9 freestream the pressure increased from 0.8 psi to 1.3 psi, roughly a 60% increase. This is plausibly a result of the shock that is formed at the nose of the store as the store moves through the shear layer and, ultimately, moves into the freestream. It should be noted for the $y = -0.5$ cm position for the Mach 2.9 condition there is an unexplained apparent low pressure region on the image. The shape of this region is the same as the shadow that was cast by the store onto the plate and is not likely an accurate measurement in this area. This shadow was present in all raw images, but the calibration and normalization process

removed them from the final result in all other cases. All images were processed in an identical manner, yet the shadow remained in this one image.
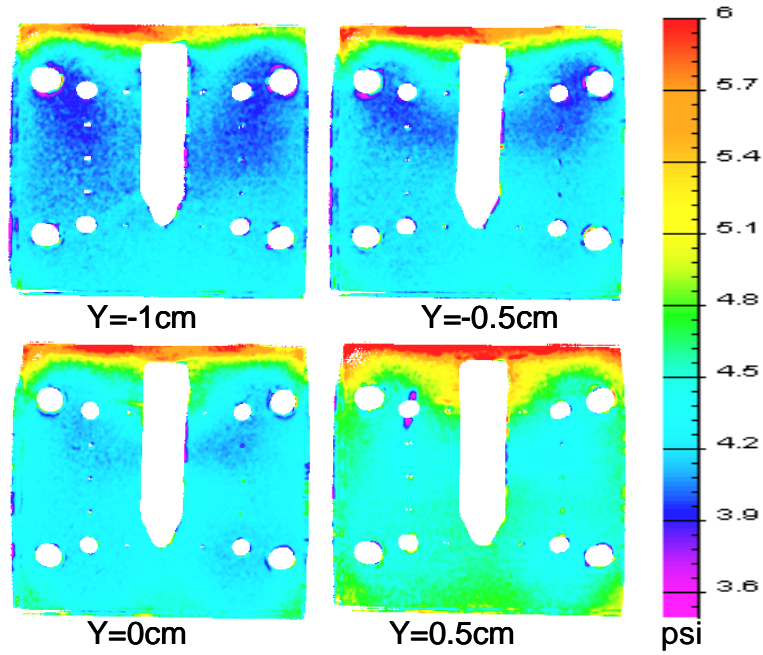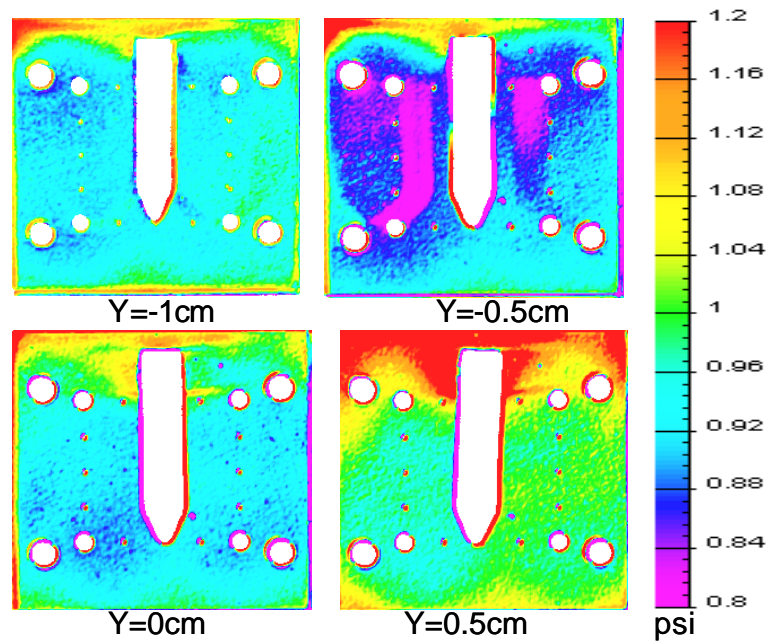
Figure 23. Effect of store position on mean pressure on cavity floor. y = 0 corresponds to store positioned at cavity edge for (a) Mach 1.8 and (b) Mach 2.9. Flow is from bottom to top.

PSP was also utilized to measure the pressure distribution on the stationary store for both conditions. Again, the floor mounted transducers were used in the calibration process. The store was placed in the lowest possible position (y = -1 cm) and, even though the pressure transducers were not directly on the surface, they were in close enough proximity to accurately calibrate the PSP. Figure 24 combines two separate views of the store. The top (freestream side) view of the store is shown in the upper portion of the figure while a perspective view, primarily taken from the side of the store, is shown in the lower portion of the figure. In each case, the store was positioned at different y-locations, as noted. Both flows exhibit the same overall trends of rising pressure on the nose of the store as it enters the shear layer and moves into the free stream.
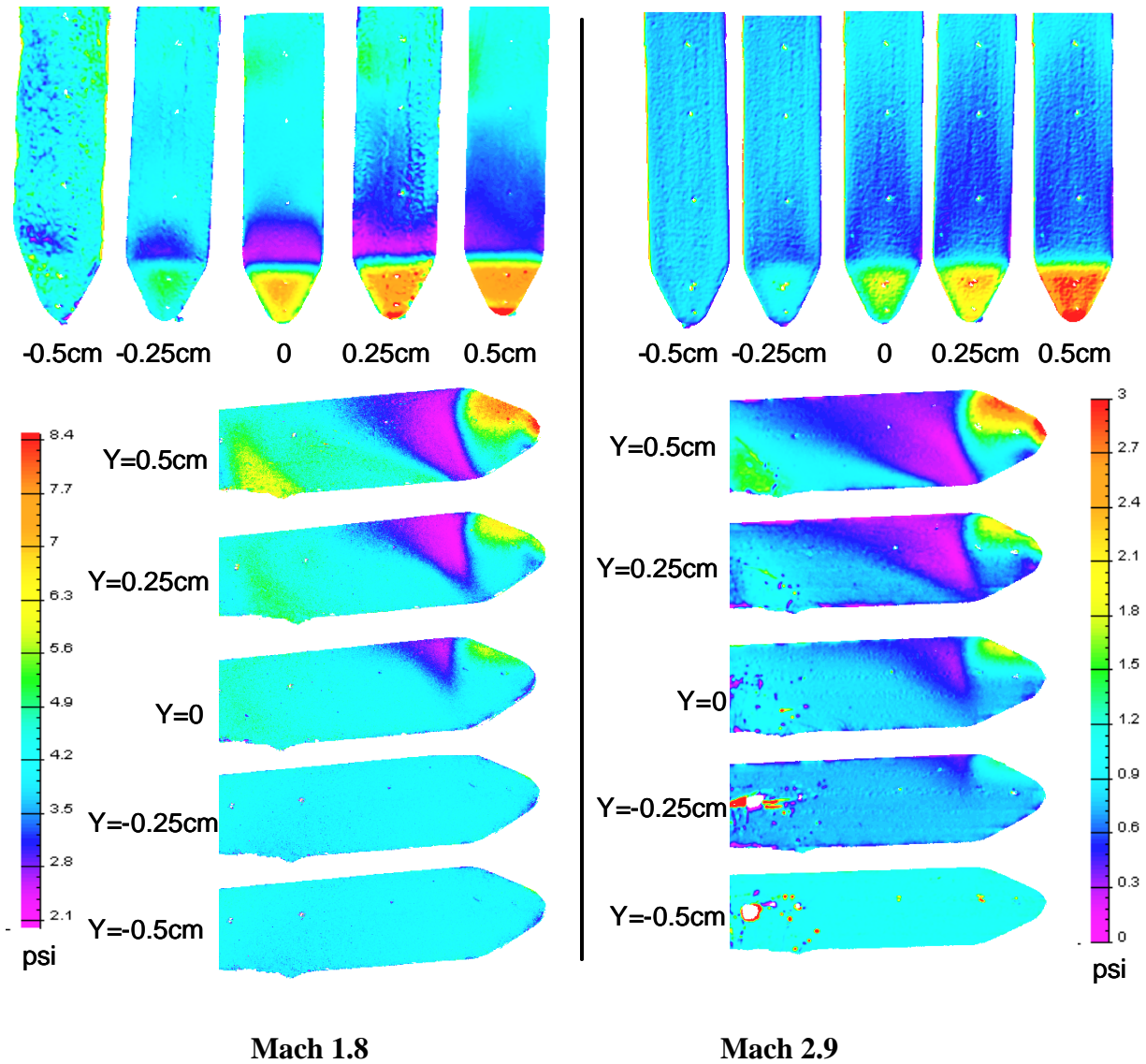
Figure 24. Effect of store position on mean pressure on the store. Side and top views of store at various heights with respect to the cavity. Top view, flow is from bottom to top. Side view, flow is from right to left.

The area of lower pressure on the cylindrical body just aft of the nose is due to the expansion fan that was visible in the Schlieren images. On the cavity-side of the nose of the store there is a small patch of lower pressure which begins when the store is at the y = 0 position. This is due to the shear layer impinging on the store. This low pressure spot

remains even though the store is moved above the shear layer. This could be further evidence of the shear layer translating away from the cavity as the store also translates away from the cavity. This corresponds well with observations of the Schlieren images. The discontinuities near the trailing edge of the store for the Mach 2.9 side view were due to lubricant contamination.

With the successful mapping of the mean pressure on the store, it was decided to go beyond the initial goals of the experiment and calculate the aerodynamic coefficients on the store to further explore the capabilities of the PSP system. Using the pressure distribution on the store at the various heights, it is a time-consuming, but straightforward process to calculate lift coefficient (C_L) and the pitching moment (C_m) on the store. The drag coefficient (C_D) is also determined, but the contribution due to the pressure which is acting on the rearward facing circular region at the trailing edge of the store was not visible with the camera position used and therefore, not included in the calculations. To distinguish this, subsequent values computed for the remaining surface is denoted C_D'. The freestream velocity, dynamic pressure, and total store surface area were used to compute the coefficients. The integration of the pressure coefficient over the surface of the store was completed using OMS 3.0 software program ProField and geometry files created by Dr. Sergey Fonov (8). It is noteworthy to discuss the experimental procedures for the calculation process. The tedious step was accurately aligning the two-dimensional PSP image with the three-dimensional geometry mesh. Since the camera position was not changed for each image acquisition, variations in position of the store as the images were recorded made each alignment different. This made it quite difficult to exactly align each image every time which produced an uncertainty of ±10% in the final calculations. Once

the images were aligned, the only additional information required by the software to perform integration process was area and length information of the store.

Due to the properties of the shear layer the trend of the aerodynamic coefficients are quite interesting. Figure 25 displays C_L for both freestream Mach numbers at various positions. A positive C_L is in the direction of pulling the store away from the cavity, where a negative C_L would be pushing the store back into the cavity. The overall trend is an increasing C_L as the store exits the cavity for both freestream Mach numbers. At the y = 0.25 cm position the Mach 1.8 case displays a large decrease in C_L. This is most certainly due to the velocity field created by the shear layer. The overall trend of increasing C_L continues as the store is moved past the shear layer into the freestream. For the Mach 2.9 case the decrease in C_L occurs at the y = 0.5 cm position. Again the shear layer is responsible for the decrease and examining the Schlieren images, it is easy to see the shear layer is higher above the cavity for the Mach 2.9 case than the Mach 1.8 case. If the store was moved to higher positions above the cavity, one would expect C_L to continue to rise until it reached a steady position when placed entirely in the freestream, away from the effects of the shear layer.
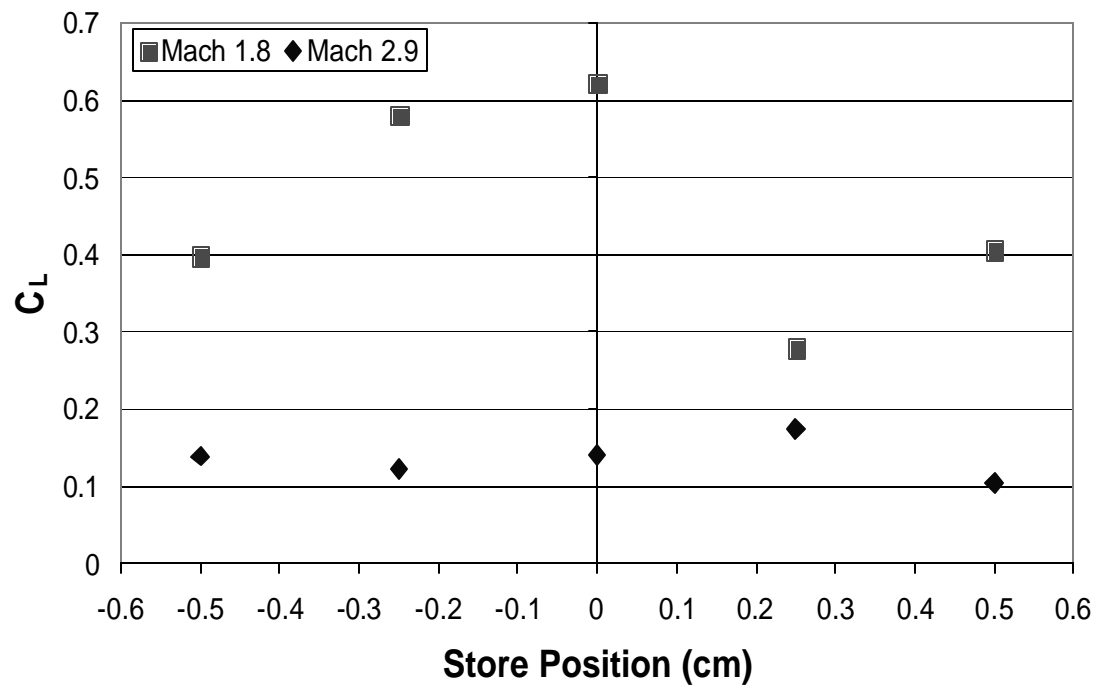
Figure 25. Lift coefficient at various store position for both freestream Mach numbers.

Figure 26 displays the results for C_D'. As expected the overall trend is an increase of C_D' as the store is moved from inside the cavity and the slower moving air, to outside the cavity and the faster moving air.
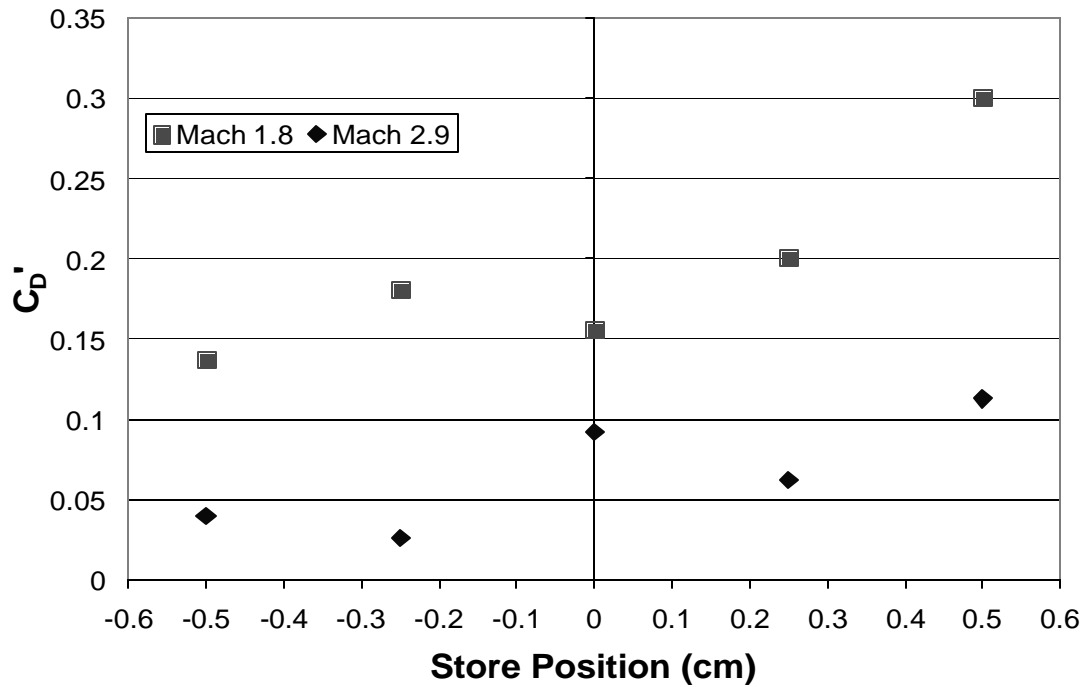
Figure 26. Drag coefficient at various store position for both freestream Mach numbers.

In Figures 27 and 28, the results of C_m are shown, with the center of moment at the nose of the store and at the center of the store, respectively. A positive moment is a counter-clockwise rotation, or the tail is rotated back into the cavity. In both figures for the Mach 2.9 flow, C_m is fairly constant at all positions, with a slight overall increase. An interesting trend occurs for the Mach 1.8 flow. In Figure 27 C_m displays a large decrease at the y = -0.25 cm and y = 0.25 cm positions. In Figure 28, C_m becomes negative for these two positions. At the y = -0.25 cm position this is most likely caused by the lack of a low pressure region formed on the upper side of the store, while the nose begins to experience a pressure rise. At the y = 0.25 cm position, the low pressure region on the upper side of the store is small in comparison to the pressure rise on the nose of the store.
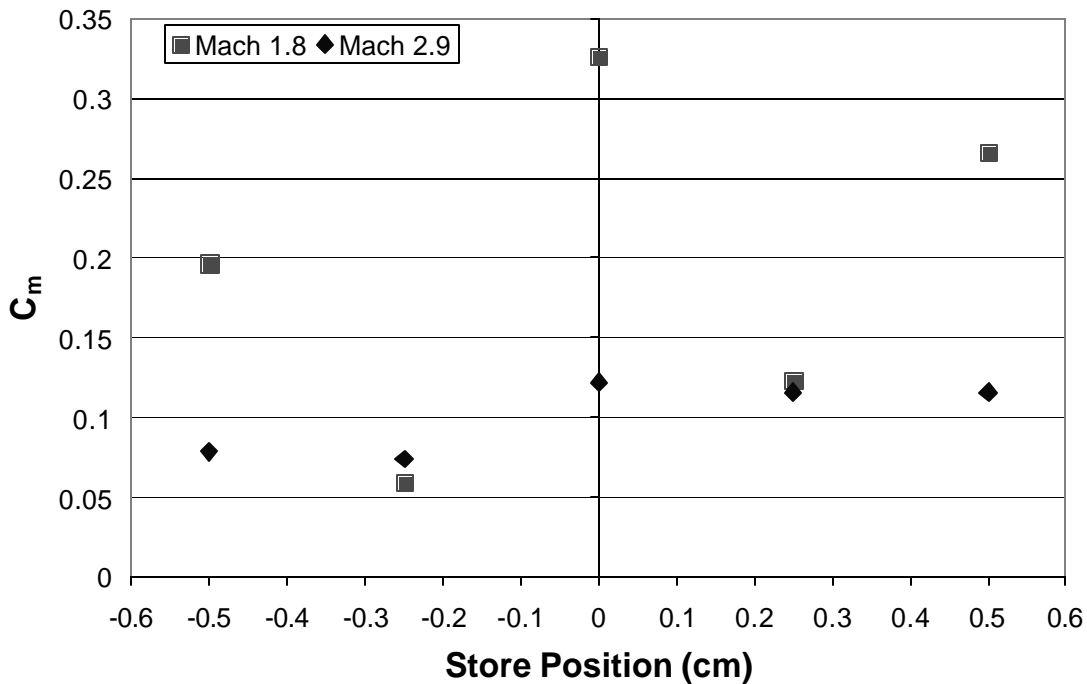
Figure 27. Pitching Moment at various store position for both freestream Mach numbers. Moment center is about nose of store.
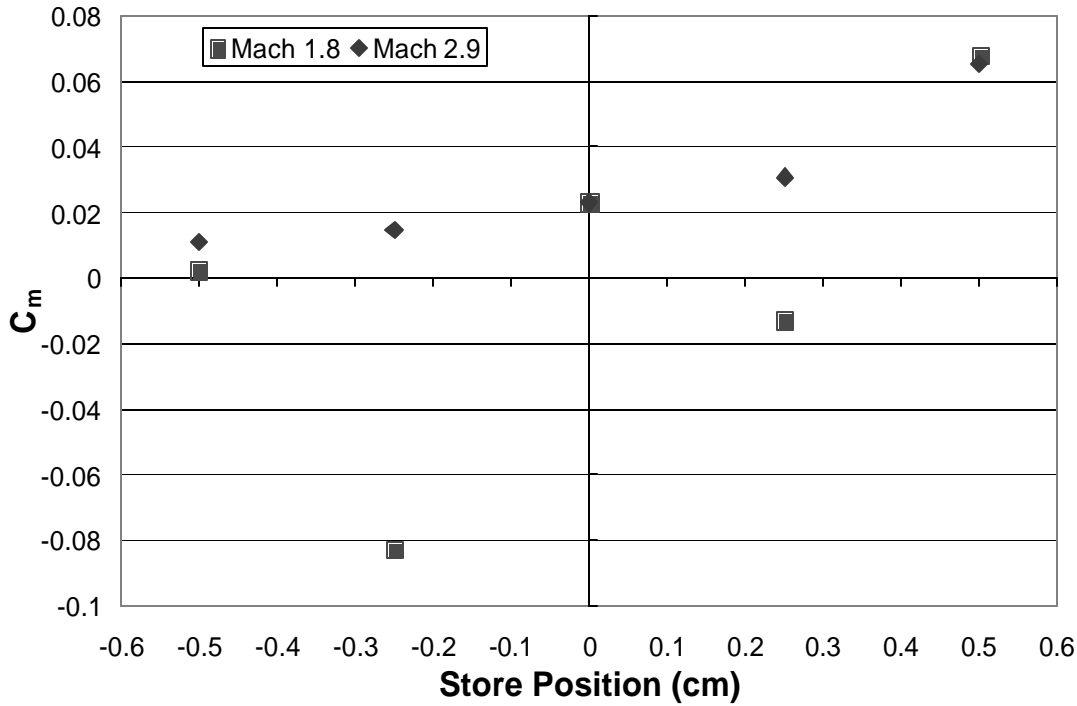
Figure 28. Pitching Moment at various store position for both freestream Mach numbers. Moment center is about center of store.

Section 2.2 - Cavity with Moving Store Present

With the effects of the stationary store on the cavity accurately characterized, a qualitative analysis of the flow about a moving store was performed using a pneumatic actuator to rapidly move the store. Upon activation, the store moved from within the cavity into the free stream in about 15 milliseconds. The images given in Figure 29 are for both freestream Mach numbers and are separated by 20 frames (1.25×10^{-3} seconds) to show the motion of the store. The starting positions of the store are the same in both columns, but the difference in appearance is from camera position and the Schlieren set-up. In this sequence, more evidence of the free shear layer rising up with the store is given. As the store exits the cavity, the shear layer appears to impinge upon the store at

the same spot, even though the store continues to move out of the shear layer. The time-response of the paint used in PSP was insufficient for applicable time-dependent pressure measurements.

(a)   (b)

Figure 29. Sequence of 12 images of a moving simulated store in freestream, (a) Mach 1.8, (b) Mach 2.9. As the store begins within the cavity (top) passes through the free shear layer (bottom). The pictures are separated by 1.25×10^{-3} seconds and are essentially uncorrelated in time, apart from the store motion. The exposure time was 1×10^{-6} seconds.

To quantify the displacement of the shear layer that is shown in Figure 29 the intensity of selected images for the Mach 2.9 freestream flow were analyzed. As shown in Figure 29(b) the dark regions characterize the shear layer, and therefore have a lower intensity level than the surrounding area. By examining the intensity on a vertical plane directly in front of the store at various store heights, it allows tracking of the lower intensity regions as shown in Figure 30. When the intensity reaches zero, the center of the shear layer has been determined. As the store starts in the cavity and begins to exit there is little displacement of the shear layer. But as the store reached $y = 2$ cm and above there is a much larger displacement of the shear layer. Between the store positions of $y = 1$ cm and $y = 3.1$ cm, the shear layer displaces approximately from $y = 0.25$ cm to $y = 0.75$ cm, roughly 0.5 cm, or a 200% increase in the position of the center of the shear layer. Schlieren images of the stationary store at different heights were also examined to ensure the shear layer displacement is caused by the presence of the store and not just the motion of the store. The results for the stationary store and the moving store were very similar and only the moving store figure is shown.

In a weapons bays where there are multiple stores released almost simultaneously, the initial stores leaving the weapons bay will traverse the shear layer and displace, encountering one type of flow structure during release, but the store that is release immediately after the first will encounter the displaced shear layer and another type of flow structure during release. Again, this can lead to the stores missing their intended target.
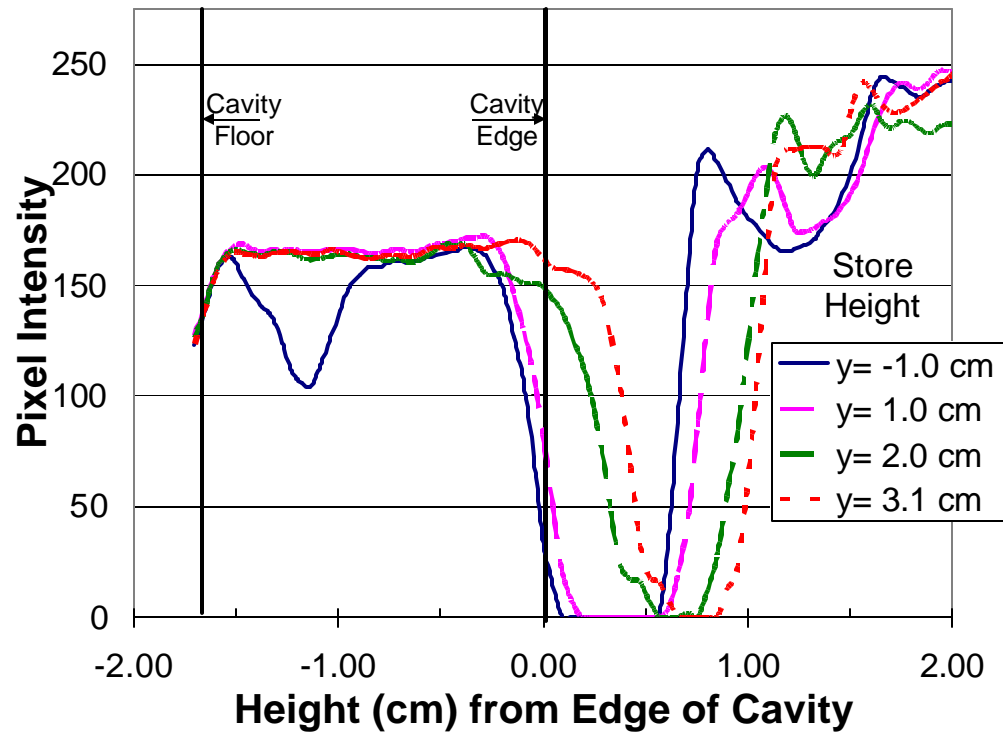
Figure 30. Displacement of shear layer as shown by changes in pixel intensity for various store heights.

V. Conclusions

Section 1 - Summary

A single cavity with a length to depth ratio of 3.6 and single store geometry were tested in AFIT's supersonic blowdown wind tunnel facility. These measurements were carried out for both a clean cavity and for a cavity containing a modeled store in order to better capture the flow physics corresponding to a weapons release. Freestream conditions of Mach 1.8 and Mach 2.9 were explored. Data was obtained with an array of high-speed pressure transducers, pressure sensitive paint (PSP), and Schlieren photography.

Stated concisely, the overall goal of this experiment is to accurately characterize aspects of the interaction of a cavity and simulated store in a supersonic freestream flow. In addition to this goal, the extensive use of PSP in this experiment vastly improved working knowledge at AFIT of the use and capabilities of PSP as a non-intrusive pressure measurement system. The experimental results gained from this experiment successfully led to increase understanding of the complex store-cavity interaction that occurs at supersonic speeds. Furthermore, this research provides benchmark global mean pressure data that could later be compared to time-accurate PSP measurements or to cases where flow control devices are implemented to alleviate the undesirable characteristics of supersonic store release from a cavity.

The initial step in achieving this goal was to characterize the clean cavity. Schlieren photography of the clean cavity indicated the three-dimensionality of the flow increased at higher Mach numbers. This observation was re-enforced by analysis of the

frequency spectra measured by transducers located on the cavity floor, which indicated the absence of a resonant peak when the freestream was Mach 2.9. PSP was also used to measure the mean pressure on the floor of the clean cavity. It revealed a pressure rise at the trailing edge of the cavity for both freestream Mach numbers.

With an understanding of the clean cavity flow field, the simulated store was placed in the cavity to gain an understanding of the interaction of the cavity and the store as a system. High-speed Schlieren images for both a stationary and a rapidly translating store were captured for both freestream conditions. In general, the visualized density gradients indicated strong fluctuations in the instantaneous pressure field, which could affect store trajectory.

The presence of a store in proximity to the cavity produced some interesting changes in the mean and fluctuating pressure on the cavity floor. In the Mach 1.8 flow, the resonant tones associated with cavity flow were present when the store was within the cavity but were eliminated when the store was placed within the free shear layer ($y = 0$). For both the Mach 1.8 and the Mach 2.9 freestream, the mean pressure levels on the cavity floor increased as the store location was shifted from within the cavity ($y < 0$) to locations outside the cavity ($y>0$). On the other hand, the standard deviation of the pressure on the cavity floor showed opposing trends, decreasing for Mach 1.8 and increasing for Mach 2.9 as the y position was increased.

PSP applied to the modeled store provided global mean pressure measurements. With reference to Figure 24, the overall pressure on the freestream side of the nose of the store is higher than on the cavity side. Downstream of the nose, the trend is opposite as

65

pressures are higher on the cavity side of the cylindrical section of the store than on the freestream side of the store.

Going beyond the initial goal of the experiment, calculations of the aerodynamic coefficients on the store revealed some interesting phenomenon. Placement of the store in the shear layer temporally disrupts the overall trend of an increase of C_L. The increase in C_L acts to pull the store away from the cavity, and needs to be taken into account when trying to predict store trajectory. As expected, C_D' increases as the store is moved from the low speed flow inside the cavity, to the high speed flow outside the cavity. For the Mach 2.9 flow, C_m is fairly constant at all positions, with a slight overall increase. For the Mach 1.8 flow, C_m displays a large decrease at the y = -0.25 cm and y = 0.25 cm positions and becomes negative at these positions when the center of moment is at the center of the store.

Schlieren images of a stationary store showed the shear layer was disrupted by the store when it was placed at or outside of the free shear layer. An objective analysis of the images indicates the shear layer shifts outward toward the store when the y-location of the store was greater than zero.

Applying these results to practical applications, the most notable is multiple store release from a cavity at supersonic speeds. The two major issues are the effect of the streamwise placement of the store and the effect of the displacement of the shear layer as the store moves through it. Both of these conditions result in different release characteristic for individual stores, making it difficult to predict the motion of every store as it exits the weapons bay and enters the freestream conditions.

66

Section 2 - Future Considerations

This experiment just touches the surface of the experimental possibilities available with the existing equipment at AFIT. The ability to configure the wind tunnel with different cavity and store geometries presents endless possibilities. Fabricating a scale model of an actual store in the military inventory today would be interesting. The ability to see the effects of a supersonic release from a cavity on an existing store could provide valuable insight on the use to the weapon in future aircraft.

The use of flow control devices would also be a logical next step. Active or passive devices could be used to control the shear layer dynamics to improve store release conditions. Several types are available and experiments with some of them could reveal the effectiveness of each type at certain freestream conditions.

PSP is a powerful pressure measurement tool available for use in a variety of experimental situations. The knowledge gained from using PSP during this experiment will allow future work at AFIT to further exploit the power of PSP in other aerodynamic experiments.

Appendix A - Additional Schlieren Images
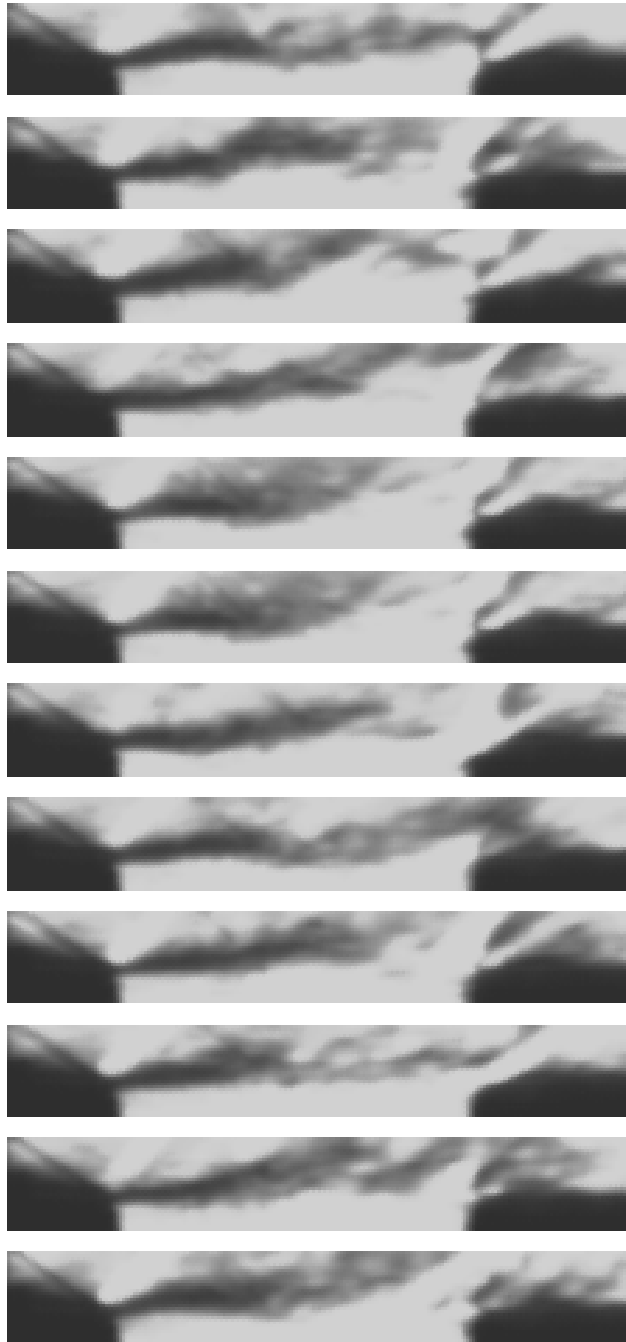
Figure 31. 12 successive Schlieren images separated by 6.25e-5 seconds characterizing the shear layer for Mach 1.8 flow. Flow is from left to right.
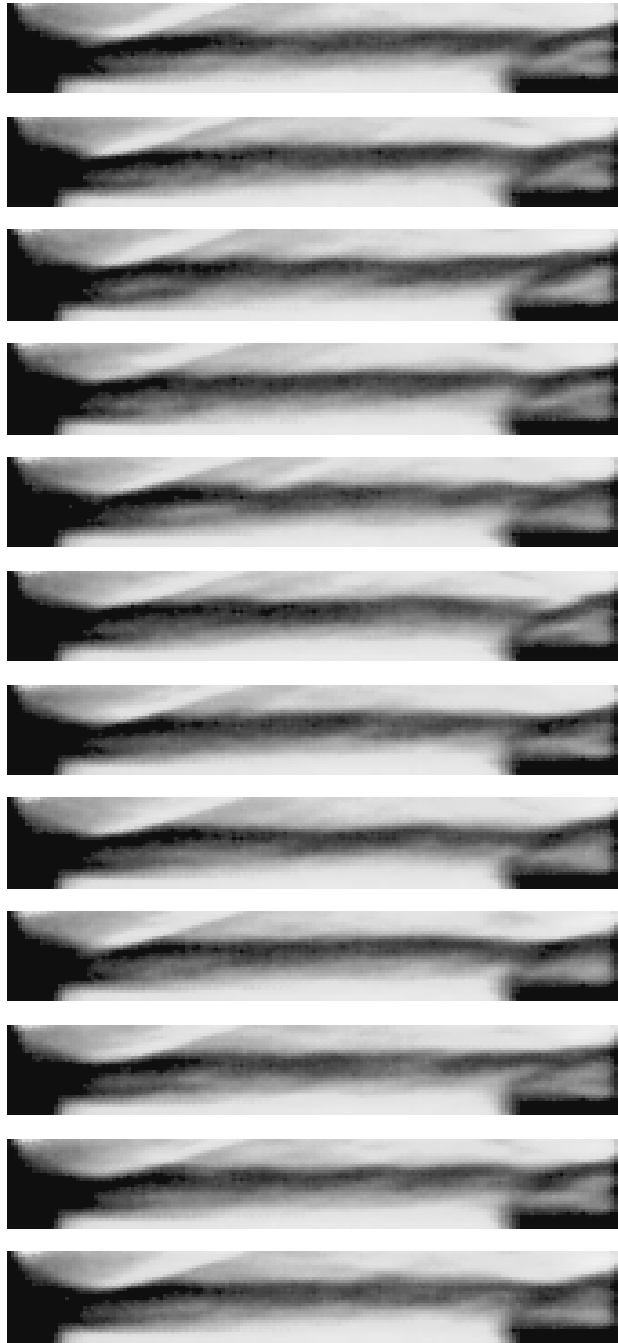
Figure 32. 12 successive Schlieren images separated by 6.25e-5 seconds characterizing the shear layer for Mach 2.9 flow. Flow is from left to right.

Appendix B - Additional Pressure Transducer Data

Table 3. Normalized Standard Deviation and Mean Pressure for all transducers for clean cavity and the store at various locations Mach 1.8.

Trans. Number	S_P/P_8	Mean P (psi)	S_P/P_8	Mean P (psi)	S_P/P_8	Mean P (psi)
1	0.0764	3.9861	0.0812	3.9939	0.0742	4.0031
2	0.0624	4.0106	0.0686	4.0341	0.0608	4.0458
3	0.2078	3.9738	0.1736	3.9692	0.1016	4.0944
4	0.1601	3.7954	0.1668	3.8206	0.1410	4.0134
5	0.1244	3.3878	0.1373	3.8448	0.1208	4.0506
Store Position	y = -1.0 cm		y = -0.5 cm		y = 0 cm	

Trans. Number	S_P/P_8	Mean P (psi)	S_P/P_8	Mean P (psi)	S_P/P_8	Mean P (psi)
1	0.0763	4.2503	0.0796	4.6046	0.06916	4.1283
2	0.0602	4.2769	0.0624	4.6214	0.0798	4.0643
3	0.0784	4.2457	0.0830	4.6137	0.1854	3.9610
4	0.1430	4.2529	0.1620	4.6101	0.1405	3.7655
5	0.1240	4.3031	0.1333	4.6624	0.1642	3.7590
Store Position	y = 0.5 cm		y = 0.8 cm		Clean Cavity	

Table 4. Normalized Standard Deviation and Mean Pressure for all transducers for clean cavity and the store at various locations Mach 2.9.

Trans. Number	S_P/P_8	Mean P (psi)	S_P/P_8	Mean P (psi)	S_P/P_8	Mean P (psi)
1	0.0872	0.8173	0.0841	0.8171	0.0913	0.8830
2	0.0316	0.9005	0.0315	0.9097	0.0340	0.9275
3	0.0568	0.8898	0.0522	0.8759	0.0474	0.9160
4	0.0675	0.8598	0.0633	0.8488	0.0786	0.9290
5	0.0495	0.8842	0.0447	0.8763	0.0497	0.9344
Store Position	y = -1.0 cm		y = -0.5 cm		y = 0 cm	

Trans. Number	S_P/P_8	Mean P (psi)	S_P/P_8	Mean P (psi)	S_P/P_8	Mean P (psi)	S_P/P_8	Mean P (psi)
1	0.0948	0.9593	0.1127	1.0775	0.0740	0.8538	N/A	N/A
2	0.0456	1.0322	0.0569	1.1646	0.0425	0.9155	N/A	N/A
3	0.0694	1.0260	0.0951	1.1767	0.0526	0.8850	0.0645	0.8963
4	0.1303	1.0515	0.1945	1.1929	0.0653	0.9107	0.0902	0.8319
5	0.0709	1.0455	0.1034	1.1925	0.0475	0.8851	N/A	N/A
Store Position	y = 0.5 cm		y = 1.0 cm		Clean Cavity		Clean Cavity 0-15 psia Trans.	

Appendix C - Pressure Transducer Specifications

SPECIFICATIONS

CERTIFIED PERFORMANCE: All specifications assume +75°F (+24°C) and 10 Vdc excitation unless otherwise stated. The following parameters are 100% tested. Calibration data, traceable to the National Institute of Standards and Technology (NIST), is supplied.

	Units	8530C-15	-50	-100
RANGE [1]	psia	0 - 15	0 - 50	0 - 100
SENSITIVITY [1]	mV/psi Typ (Min)	15.0 (9.3)	4.5 (2.8)	2.25 (1.4)
COMBINED: NON-LINEARITY, NON-REPEATABILITY, PRESSURE HYSTERESIS [2]	% FSO RSS Max	0.50	0.40	0.40
Non-Linearity, Independent	% FSO Typ	0.15	0.1	0.1
Non-Repeatability	% FSO Typ	0.1	0.1	0.1
Pressure Hysteresis	% FSO Typ	0.1	0.1	0.1
ZERO MEASURAND OUTPUT [3]	mV Max	±20	±20	±20
ZERO SHIFT AFTER 3X RANGE	±% 3X FSO Max	0.2	0.2	0.2
THERMAL ZERO SHIFT From 0°F to 200°F (-18°C to +93°C)	±% FSO Max	3	3	3
THERMAL SENSITIVITY SHIFT From 0°F to 200°F (-18°C to +93°C)	±% Max	3	3	3

	Units	8530C-15	-50	-100
RESONANCE FREQUENCY	Hz	180 000	320 000	500 000
NON-LINEARITY AT 3X RANGE	% 3X FSO	1.0	1.0	1.0
ZERO SHIFT WITH MOUNTING TORQUE 15 lbf-in. (1.7 Nm)	% FSO	0.2	0.5	0.5
THERMAL TRANSIENT RESPONSE PER ISA-S37.10, PARA. 6.7, PROCEDURE I [4]	psi/°F	0.003	0.003	0.010
	psi/°C	0.005	0.005	0.018
PHOTOFLASH RESPONSE [5]	Equiv. psi	0.1	0.3	0.6
WARM-UP TIME [6]	ms	1	1	1
ACCELERATION SENSITIVITY	Equiv. psi/g	0.00015	0.00015	0.00015
BURST PRESSURE (Diaphragm)	psia Min	75	250	400
CASE PRESSURE [7]	psia Min	1000	1000	1000

ELECTRICAL

FULL SCALE OUTPUT	225 mV typical (140 mV minimum) at 10.0 Vdc
SUPPLY VOLTAGE [8]	10.0 Vdc recommended, 15 Vdc maximum
ELECTRICAL CONFIGURATION	Active four-arm piezoresistive bridge
POLARITY	Positive output for increasing pressure
RESISTANCE	
Input	2600 ohms typical, 1700 ohms minimum
Output	1500 ohms typical, 2200 ohms maximum
Isolation	100 megohms minimum at 50 Volts; leads to case, leads to shield, shield to case
NOISE	5 microvolts rms typical, dc to 50 000 Hz; 50 microvolts rms maximum, dc to 50 000 Hz

MECHANICAL

CASE, MATERIAL	Stainless Steel (17-4 PH CRES)
CABLE, INTEGRAL	Four conductor No. 32 AWG Teflon® insulated leads, braided shield, gray silicone jacket, 30 ±6 in (760 ±150mm)
DEAD VOLUME (+) PORT	0.0003 cubic inches (0.005 cc)
MOUNTING/TORQUE	10-32 UNF-2A threaded Case 0.438 inch (11.12 mm) long/15 ± 5 lbf-in (1.7 ±0.6 Nm)
WEIGHT	2.3 grams (cable weighs 9 grams/meter)

ENVIRONMENTAL

MEDIA [9]	Internal seals are epoxy compatible with clean dry gas media. Media is exposed to CRES, ceramic, silicon, Parylene C, epoxy, silicone rubber, and the O-Ring. For use in water or corrosive media, contact the factory for modifications and installation precautions which may be taken to extend service life
TEMPERATURE [10]	-65°F to +250°F (-54°C to +121°C)
VIBRATION	1000 g pk
ACCELERATION	1000 g
SHOCK	20 000 g, 100 microsecond haversine pulse
HUMIDITY	Isolation resistance greater than 100 megohms at 50 volts when tested per MIL-STD-202E, Method 103B, Test Condition

Figure 33. Endevco Pressure Transducer Specifications.

Bibliography

1. Anderson, John D., *Modern Compressible Flow, Third Edition,* McGraw Hill Publishing, 2003, pp 127-160.

2. Baysal, O., Fouladi, K., Leung, R. and Sheftic, J., "Interference Flows Past Cylinder-Fin-Sting-Cavity Assemblies," AIAA Journal of Aircraft, March 1992, Vol. 29, No. 2, pp. 194-202.

3. Bell, J.H., Schairer, E.T., Hand, L.A., and Mehta, R., "Surface Pressure Measurements Using Luminescent Coating", Annual Review of Fluid Mechanics, 2001, Vol. 33, pp. 155-206.

4. Brock, James, M. and Lutton, Mark, "Applies computational Fluid Dynamics in Support of Aircraft and Weapons Integration," Online publication (19 August 1999), 27 January 2004 http//www.hpcmo.hpc.mil/Htdoc/UGC/UGC99/paperspchal3-3/

5. Bueno, P., Unalmis, O., Clemens, N., Dolling, D., "The Effects of Upstream Mass Injection on a Mach 2 Cavity Flow," *AIAA Paper* 2002-0663.

6. Cattafesta, L., Williams, D., Rowley, C., and Alvi, F., "Review of Active Control of Flow-Induced Cavity Resonance," *AIAA Paper* 2003-3567.

7. Crites, R.C., "Measurement Techniques: Pressure Sensitive Paint Technique," *von Karman Institute for Fluid Dynamic,* Lecture Series 1995-01.

8. Fonov, S., Team Leader, Optical Measurements, Innovative Scientific Solutions Incorporated, Personal Correspondence and Computer files, 10 February, 2004.

9. Grove, J., Shaw, L., Leugers, J., Akroyd, G., "UASF/RAAF F-111 Flight Test with Active Separation Control," *AIAA Paper* 2003-0009.

10. Hamed, D., Basu, A., Mohamed, A., and Das, K., "Detached Eddy Simulations of Supersonic Flow Over Cavity," *AIAA Paper* 2003-0549.

11. Hamed, D., Basu, A., Mohamed, A., and Das, K., "Direct Numerical Simulations of High Speed Flow Over Cavity," AFOSR Conference Paper, presented at 3rd AFOSR International Conference on DNS/LES, 2001.

12. Heller, H.H., Holmes, D.G., and Covert, E.E, "Flow Induced Pressure Oscillations In Shallow Cavities," *Journal of Sound and Vibration*, Vol. 18, No. 4, 1971, pp. 545-553.

13. McIntyre, Thomas, C., "Flow Field and Loading Analysis on a Wrap-Around Fin Missile," MS Thesis, AFIT/GAE/ENY/97D-04. School of Engineering and Management, Air Force Institute of Technology (AU), Wright-Patterson AFB OH, December 1997.

14. Morris, M.J., Donovan, J.F., Kegelman, J.T., Schwab, S.D., and Levy, R.L., "Aerodynamic Applications of Pressure-Sensitive Paint," *AIAA Paper* 1992-0264, January, 1992.

15. Mosbarger, N.A. and King, P.I., 1996, "Time-Dependent Supersonic Separation of Tangent Bodies," *Journal of Aircraft*, Vol. 33, No. 5, pp. 938-949.

16. Murray, R., and Elliott, G., "Characteristics of the Compressible Shear Layer over a Cavity," *AIAA Journal*, Vol. 39, No. 5, May 2001, pp. 846-856.

17. Perng, S.W. and Dolling, D.S., "Suppression of Pressure Oscillations in High-Mach-Number Turbulent, Cavity Flow," *Journal of Aircraft*, Vol. 38, No. 2, 2001, pp. 248-256.

18. Powell, Orval, A., "Heat Transfer to the Inclined Trailing Wall of an Open Cavity," MS Thesis, AFIT/GAE/ENY/97D-04. School of Engineering and Management, Air Force Institute of Technology (AU), Wright-Patterson AFB OH, December 1997.

19. "Pressure Sensitive Paints: Products," ISSI Company website, 19 August 2003 http://innssi.com/psp/index_products_psp_unifib.htm.

20. "Pressure Sensitive Paints: Summary," ISSI Company website, 19 August 2003 http://innssi.com/psp/index_products_psp_Summary.htm.

21. Reeder, M., Subramanian, C., "Mean and Instantaneous flow Properties of An Object Exiting a Cavity," *AIAA Paper* 2003-3723.

22. Rockwell, D. and Naudascher, E., "Review – Self-Sustaining Oscillations of Flow Past Cavities," *Journal of Fluids Engineering*, Vol. 100, June 1978, pp. 152-165.

23. Rossiter, J.E., "Wind-Tunnel Experiments on the Flow over Rectangular Cavities at Subsonic and Transonic Speeds," *Aeronautical Research Council Reports and Memoranda 3438*, 1964.

24. Samimy, M. and Kastner, J., "Effects of Forcing Frequency on the Control of an Impinging High Speed Jet," *AIAA Paper* 2003-0006.

25. Sarno, R., Franke, M., "Suppression of Flow-Induced Pressure Oscillations in Cavities," *Journal of Aircraft*, Vol. 31, No. 1, 1994, pp. 90-96.

26. Schindel, L.H., "Store Separation," *Advisory Group for Aerospace Research & Development (AGARD),* AGARDograph No. 202, 1975.

27. Schlichting, Herman, *Boundary-Layer Theory, Seventh Edition*, McGraw-Hill Publishing, 1979, pp 5-45.

28. Settles, G.S., *Schlieren and Shadowgraph Techniques*, Springer Publishing, 2001, pp 39-75.

29. Shalaev, V.I., Fedorov, A.V., and Malmuth, N.D., 2001, "Dynamics of Slender Bodies Separating from Rectangular Cavities," *AIAA Journal*, Vol. 40, No. 3, March 2002, pp. 517-525.

30. Smith, B., Welterlen, T., Maines, B., Shaw, L., Stanek, M., and Grove, J., "Weapons Bay Acoustic Suppression from Rod Spoilers," *AIAA Paper* 2002-0662.

31. Stallings, Robert L. & Wilcox, Floyd, J., "Experimental Cavity Pressure Distributions at Supersonic Speeds," NASA Technical Paper 2683, 1987.

32. Stanek, M., Raman, G., Kibens, V., Ross, J., Odedra, J., and Peto, J., "Control of Cavity Resonance Through Very High Frequency Forcing," *AIAA Paper* 2000-1905.

33. Ukeiley, L., Ponton, M., Seiner, J., and Jansen, B., "Suppression of Pressure Loads in Cavity Flows," *AIAA Paper* 2002-0661.

34. Unalmis, O.H., Clemens, N.T., and Dolling, D.S., "Experimental Study of Shear-Layer/Acoustics Coupling in Mach 5 Cavity Flow," *Journal of Aircraft*, Vol. 39, No. 2, February 2001, pp. 242-252.

35. Wilcox Jr., Floyd J., Baysal, Oktay, and Stallings Jr., Robert L., "Tangential, Semisubmerged, and Internal Store Carriage and Separation", *Tactical Missile Aerodynamics: General Topics*, Vol. 141. Chapter 14, 1992, pp 667-721.

36. Williams, D.R., Fabris, D., Morrow, J., "Experiments on Controlling Multiple Acoustic Modes in Cavities," *AIAA Paper* 2000-1903.

37. Zhang, X. and Edwards, J.A., "An Investigation of Supersonic Oscillatory Cavity Flows Driven by Thick Shear Layers," *Aeronautical Journal*, December 1990, pp. 355-364.

Vita

Scott Bjorge was raised in Ridgeway, Wisconsin. He attended Dodgeville High School in Dodgeville, Wisconsin. He accepted a ROTC scholarship to attend the University of Wisconsin-Madison where he earned a Bachelor of Science Degree in Mechanical Engineering. Upon commissioning Scott was stationed at Mountain Home AFB, Idaho, where he was an Aircraft Maintenance Officer for several squadrons, including the 34th Bomb Squadron "Thunderbirds". Scott is an avid sports fan and enjoys hanging out with his dogs and spending time outside.

REPORT DOCUMENTATION PAGE

1. REPORT DATE *(DD-MM-YYYY)*	**2. REPORT TYPE**	**3. DATES COVERED** *(From – To)*
04-03-2004	Master's Thesis	August 2002 – March 2004

4. TITLE AND SUBTITLE		
FLOW AROUND AN OBJECT PROJECTED FROM A CAVITY INTO A SUPERSONIC FREESTREAM	**5a. CONTRACT NUMBER**	
	5b. GRANT NUMBER	
	5c. PROGRAM ELEMENT NUMBER	
6. AUTHOR(S)	**5d. PROJECT NUMBER** 2003-024	
Scott T. Bjorge, Captain, USAF	**5e. TASK NUMBER**	
	5f. WORK UNIT NUMBER	

7. PERFORMING ORGANIZATION NAMES(S) AND ADDRESS(S)	**8. PERFORMING ORGANIZATION REPORT NUMBER**
Air Force Institute of Technology Graduate School of Engineering and Management (AFIT/EN) 2950 Hobson Way, Building 640 WPAFB OH 45433-8865	AFIT/GAE/ENY/04-M02

9. SPONSORING/MONITORING AGENCY NAME(S) AND ADDRESS(ES)	**10. SPONSOR/MONITOR'S ACRONYM(S)** AFRL/MN
Air Force Research Laboratory/Munitions Directorate Bldg 13 Eglin AFB, FL 32542	**11. SPONSOR/MONITOR'S REPORT NUMBER(S)**

12. DISTRIBUTION/AVAILABILITY STATEMENT

APPROVED FOR PUBLIC RELEASE; DISTRIBUTION UNLIMITED.

13. SUPPLEMENTARY NOTES

14. ABSTRACT

The pressure and flow field of a supersonic flow over a cavity, with and without a store, was the focus of this experiment. One cavity geometry (length to depth ratio 3.6) was studied, the freestream Mach number and the placement of the store relative to the cavity floor were varied.

The pressure spectra on the cavity floor were markedly different between Mach numbers of 1.8 and 2.9. The Mach 1.8 case exhibited clear spectral peaks consistent with predictions by Rossiter, the Mach 2.9 flow did not. With the store placed within the free shear layer, the pressure fluctuations on the cavity floor decreased for Mach 1.8 and increased for Mach 2.9.

High-speed Schlieren photography was used visualize the interaction of the free shear layer and the modeled store. Images revealed that flow structures in the free shear layer of the Mach 2.9 flow exhibited less spanwise coherence then their Mach 1.8 flow counterparts. Images also revealed vertical displacement of the free shear layer as the store traversed through it.

Pressure-sensitive paint (PSP) was utilized to quantify the full-field mean pressure on the cavity floor and store. A pressure rise near the trailing edge was noted for both freestream Mach numbers. The mean pressure contour of the floor for the Mach 1.8 exhibited considerable three-dimensionality, despite the generally spanwise coherent structures in the free shear layer.

15. SUBJECT TERMS

Cavity Flow, Store Separation, Pressure Sensitive Paint

16. SECURITY CLASSIFICATION OF: UNCLASSIFIED			**17. LIMITATION OF ABSTRACT**	**18. NUMBER OF PAGES**	**19a. NAME OF RESPONSIBLE PERSON** Dr. Mark F. Reeder
a. REPORT	**b. ABSTRACT**	**c. THIS PAGE**			**19b. TELEPHONE NUMBER** *(Include area code)*
U	U	U	UU	90	(937) 255-3636, ext 4530 (mark.reeder@afit.edu)